*Article*

# Human Papillomavirus 16 E6 and E7 Oncoproteins Alter the Abundance of Proteins Associated with DNA Damage Response, Immune Signaling and Epidermal Differentiation

Kerry Dust [1,2], Michael Carpenter [3], Julie Chih-yu Chen [3], Chris Grant [3], Stuart McCorrister [3], Garret R. Westmacott [3] and Alberto Severini [1,3,*]

[1] Department of Medical Microbiology, Faculty of Health Sciences, University of Manitoba, Winnipeg, MB R3E 0W2, Canada
[2] Cadham Provincial Laboratory, Manitoba Health, Winnipeg, MB R3C 3J7, Canada
[3] National Microbiology Laboratory, Public Health Agency of Canada, Winnipeg, MB R3E 3M4, Canada
* Correspondence: alberto.severini@phac-aspc.gc.ca; Tel.: +1-1204-789-6022; Fax: +1-204-318-2222

**Abstract:** The high-risk human papillomaviruses are oncogenic viruses associated with almost all cases of cervical carcinomas, and increasing numbers of anal, and oral cancers. Two oncogenic HPV proteins, E6 and E7, are capable of immortalizing keratinocytes and are required for HPV associated cell transformation. Currently, the influence of these oncoproteins on the global regulation of the host proteome is not well defined. Liquid chromatography coupled with quantitative tandem mass spectrometry using isobaric-tagged peptides was used to investigate the effects of the HPV16 oncoproteins E6 and E7 on protein levels in human neonatal keratinocytes (HEKn). Pathway and gene ontology enrichment analyses revealed that the cells expressing the HPV oncoproteins have elevated levels of proteins related to interferon response, inflammation and DNA damage response, while the proteins related to cell organization and epithelial development are downregulated. This study identifies dysregulated pathways and potential biomarkers associated with HPV oncoproteins in primary keratinocytes which may have therapeutic implications. Most notably, DNA damage response pathways, DNA replication, and interferon signaling pathways were affected in cells transduced with HPV16 E6 and E7 lentiviruses. Moreover, proteins associated with cell organization and differentiation were significantly downregulated in keratinocytes expressing HPV16 E6 + E7. High-risk HPV E6 and E7 oncoproteins are necessary for the HPV-associated transformation of keratinocytes. However their influence on the global dysregulation of keratinocyte proteome is not well documented. Here shotgun proteomics using TMT-labeling detected over 2500 significantly dysregulated proteins associated with E6 and E7 expression. Networks of proteins related to interferon response, inflammation and DNA damage repair pathways were altered.

**Keywords:** human papillomavirus; E6 protein; E7 protein; proteomics; keratinocytes; transformation

## 1. Introduction

Human papillomaviruses (HPV) are small, non-enveloped DNA viruses, which infect epithelial keratinocytes. These viruses are transmitted by physical contact, resulting in warts, hyperplastic lesions and, in some cases, cancer [1]. Of the hundreds of types of HPV, there is a small group classified as high-risk for their association with oropharyngeal and anogenital cancer by the International Committee on Taxonomy of Viruses [2].

Although most infections with HPV are cleared by the host within two years, infections which persist pose a high risk for carcinogenesis [3]. The long-term expression of high-risk HPV E6 and E7 oncoproteins promote immortalization and transformation of keratinocytes but the exact mechanism by which this occurs is not completely known [4,5]. The ability of high-risk HPV oncoproteins E6 and E7 to bind and degrade the host tumor suppressor proteins retinoblastoma (pRb) and p53 to promote viral replication and prevent

host apoptosis is well-established [6–9]. Additionally, the E6 and E7 oncoproteins are known to degrade, mislocalize or activate many other host proteins [10–13]. A thorough characterization of the global dysregulation of the host proteome and signaling pathways affected by HPV16 E6 and E7 would clarify the roles of the E6 and E7 oncoproteins in HPV biology and determine how these viruses evade immune detection. It would additionally illuminate the mechanisms that foster persistence and lead to transformation.

Previous investigations into the effects of HPV infection revealed altered protein expression signatures compared to uninfected or non-cancerous tissues [14–18]. Unfortunately, most of these studies used cancerous cells or tissues and using such a heterogeneous population of cells to study proteomic changes dampens the power of those investigations to discern the effects of viral proteins on the host proteome. Additionally, any differential protein levels observed in HPV infected tissues cannot be specifically attributed to the E6 and E7 proteins. There have been previous studies investigating the effects of HPV16 E6 or HPV16 E6 and E7 on the host proteome using two-dimensional difference gel electrophoresis followed by mass spectrometry. However the limited sensitivity of gel based proteomic methods may explain the scarcity of deregulated proteins associated with those studies [19] Current shotgun proteomics analysis by liquid chromatography-tandem mass spectrometry (LC-MS/MS) coupled with pathway analysis promise enhanced sensitivity for the exploration of the global dysregulation of the host proteome by full-length HPV16 E6 and E7 proteins [20].

To catalogue the differential abundance of critical proteins altered in primary keratinocytes expressing full-length HPV16 E6 and E7 proteins, we employed gel free, liquid chromatography coupled with tandem mass spectrometry for a shotgun proteomics analysis. The use of isobaric tags is a well-established method for measuring differential protein levels between samples [20].

Here we provide a glimpse into the global proteomic alterations resulting from the presence of HPV oncoproteins. Canonical signaling pathways related to DNA damage response, DNA replication and interferon signaling pathways were affected in cells transduced with lentiviruses encoding HPV16 E6 and E7 genes. In addition, proteins associated with cell organization and differentiation were significantly downregulated in keratinocytes expressing HPV16 E6 and E7.

## 2. Methods

### 2.1. Cell Culture

Primary human neonatal keratinocytes (HEKn) (Life Technologies, Grand Island, NE, USA, cat# C0015C) were grown in Epilife media (Life Technologies, Grand Island, NE, USA, cat# MEPI500CA) supplemented with 1% human keratinocyte growth serum (HKGS) (Life Technologies, Grand Island, NE, USA, cat# S0015). Cultures were maintained at 37 °C in a humidified incubator at 5% $CO_2$.

### 2.2. Lentivirus Production

A splice mutant of the HPV16 E6 gene (Genbank Accession# NC_001526) was constructed with a point mutation (nt 227 G→A) that abolishes the 5′ splice site to promote the expression of full- length E6 proteins. Truncated E6 proteins resulting from the splice site do not have the same biological capacity for transformation as the full length E6 proteins [21].

This splice-mutant HPV16 E6 gene was inserted into pCDH-CMV-MCS-EF1-Neo (Systems Biosciences, Palo Alto, CA, USA, cat# CD514B-1) lentivector, and an HPV16 E7 gene was inserted into pCDH-CMV-MCS-EF1-Hygro (Systems Biosciences, Palo Alto, CA, USA, cat# CD515B-1) lentivector.

293TN cells (Systems Biosciences, Palo Alto, CA, USA, cat#LV900A-1) were transfected with 1 mL DMEM, lentivector and packaging plasmids: pPACKH1-GAG, pPACKH1-REV, and pVSV-G along with 30 μL of Roche Xtreme gene HP (Roche, Mississauga, ON, Canada cat# 06366236001). The transfected 293TN cells were maintained in DMEM (Life Technologies, Grand Island, NE, USA, cat#11966-025) supplemented with 4 mM L-glutamine, 4 g/L

glucose, 100 units/mL penicillin-G, 100 µg/mL streptomycin (90%) and 10% fetal bovine serum (FBS) for 48 h at 37 °C in a humidified incubator at 5% $CO_2$.

Lentiviruses were harvested from the tissue culture supernatant, mixed with PEG-it™ viral precipitation solution (System Biosciences, Palo Alto, CA, USA, cat# LV810A-1) and stored at 4 °C overnight to concentrate the virus. The next day the lentiviruses were pelleted by centrifugation at $1500 \times g$ for 40 min at 4 °C. The pellet was resuspended in 1/10 the volume of DMEM supplemented with 2% FBS.

### 2.3. Lentiviral Titration

To determine the lentiviral titer, the number of functional lentiviral particles was measured by qPCR of the lentivector Woodchuck Hepatitis Virus Posttranscriptional Regulatory Element following infection of HEKn cells [22]. GAPDH was used for normalization. DNA was extracted from infected cells 48 h post-infection using the Qiagen QIAamp DNA mini kit (Qiagen, Germantown, TN, USA, cat# 51304) as per the manufacturer's instructions. In each 20 µL reaction, 0.4 µM of each primer (WPRE Forward: CGCTGCTTTAATGC-CTTTGTAT; WPRE Reverse: GGGCCACAACTCCTCATAAA) was added to 10 µL of SYBR green master mix (Biotool.com cat# B21203). A Roche 480 Lightcycler (Roche Life Sciences Inc., Indianapolis, IN, USA) was used for DNA amplification. Cycling conditions were as follows: one cycle of 50 °C for 2 min, one cycle of 95 °C for 2 min, 40 cycles of 95 °C for 3 s and 60 °C for 30 s. Similarly, for GAPDH amplification 0.4 µM of primers and 10 µL of SYBR green were used in each 20 µL reaction PCR: (GAPDH Forward: ACATCGCTCA-GACACCATG; GAPDH reverse: TGTAGTTGAGGTCAATGAAGGG). The titer of each sample was then determined by calculating the amount of WPRE element relative to that of GAPDH DNA against a standard curve that was generated from serially diluted WPRE DNA quantified standards.

### 2.4. Transduction

HEKn cells at approximately 25 population doublings were seeded into 24 well culture plates (Corning, Corning, NY, USA, cat# 3524) at 25,000 cells per well. HEKn cells were transduced with both HPV16 E6 and E7 lentiviruses at an MOI of one. For controls, HEKn cells were transduced with lentiviruses created with unmodified lentivectors (LV-HEKn). Four biological replicates were performed for the HPV16 E6 and E7, and the LV-HEKn transductions. To control for transduction, and antibiotic selection, HEKn cells were transduced with lentiviruses carrying a Green Fluorescent Protein (GFP) insert. The transduced cells were incubated at 37 °C in 5% $CO_2$. Antibiotic selection was started at the first media change, 48 h post-transduction. Initially, 15 µg/mL Gibco Geneticin G418 Sulfate (Thermo Fisher Scientific, Waltham, MA, USA, cat # 10131035) and 15 µg/mL Hygromycin B (Thermo Fisher Scientific, Waltham, MA, USA, cat # 10687010) were used for five days. Then, 5 µg/mL of each were used for ten days to ensure the elimination of cells not containing a lentivirus insertion. Four biological replicates were performed in a similar manner.

The presence of HPV16 E6 and E7 mRNA was verified by RT-PCR. First E6 and E7 mRNA was extracted from the transduced cells using Qiagen's RNeasy kit (Qiagen cat# 74104) as per the manufacturer's instructions. Each RT-PCR reaction consisted of 5 µL of TaqMan® Fast Virus 1-Step Master Mix (TFV) (Thermo Fisher cat# 4444432), 6 µL of water and 1 nM each HPV16_E6 primers forward: CCATGCACCAAAAGAGAACTG and HPV16_E6 reverse: TCAGGACACAGTGGCTTTTGA, 5 µL of 10 ng/µL RNA. Amplification was achieved with the following conditions: 50 °C for 5 min, 95 °C for 20 s followed by 40 cycles of 95 °C for 3 s and 55 °C for 30 s. Similarly, E7 mRNA was identified using HPV16_E7 primers forward: ACATGGA TCCGCCACCATGCAT GGA-GATACACC and HPV16_E7 reverse ATGTGCGGCCGCTTATTATGGTTTCTGAG. The bands were visualized using a Qiaxcel High-Resolution DNA kit (Qiagen cat# 929002) as per the manufacturer's instructions.

## 2.5. Protein Harvest and Quantification

After selection with antibiotics, transduced cells were grown to confluence in T75 flasks. After 45 population doublings cells were harvested. Epilife media was removed and the cells were washed twice with cold PBS. Next, the cells were manually scraped from the flasks and collected in 2% Sodium dodecyl sulfate (SDS) in Phosphate-buffered saline (PBS). Cells in 2% SDS were heated for 5 min at 99 °C and then homogenized using Qiashredder column as per the manufacturer's instructions (Qiagen, Germantown, TN, USA, cat#79656). Proteins were quantified using a Pierce BCA kit as per the manufacturer's instructions (Pierce, Rockford, IL, USA, cat #23227).

## 2.6. Peptide Digestion and Tandem Mass Tag (TMT) Labeling

To prepare the peptides for mass spectrometry, 100 μg of proteins were combined 1:10 with 1 M Dithiothreitol (DTT) (Sigma Aldrich, St. Louis, MO, USA, cat# DO632) and heated for 5 min at 99 °C to reduce disulfide bonds. Once cooled to room temperature the sample was incubated with an equal volume of urea exchange buffer (UEB) at room temperature for 10 min. UEB is 8 M Urea (GE Healthcare, Chicago, IL, USA, cat# 17-1319-01) in 50 mM HEPES buffer (Thermo Fisher Scientific, Waltham, MA, USA, cat# 15630106). Nanosep 10 K Omega filter cartridges (PAL Life Sciences Port, Washington, DA, USA, cat# OD010C34) were prepared by adding 200 μLwater to the filter and centrifuging 10,000× $g$ for 3 min followed by 200 μLUEB to the filter cartridge and centrifuge 10,000× $g$ for 3 min. The samples were applied to the filter cartridge and centrifuged 10,000× $g$ for 3 min × $g$ for 10–15 min. The filter cartridge was washed 3 times by adding 250 μLUEB and centrifuging at 10,000× $g$ for 10–15 min for each wash. After the third wash 100 μL of 50 mM Iodoacetamide (IAA) (Sigma Aldrich, St. Louis, MO, USA, cat# I6125) solution was added to the cartridge, the samples shaken at 600 rpm for 1 min, then placed in the dark for 20 min. The samples were then centrifuged at 10,000× $g$ for 10–15 min. The filter cartridges were washed three times by adding 100 μLUEB and centrifuging at 10,000× $g$ for 10–15 min for each wash. The samples were further washed by adding 150 μL Ammonium Bicarbonate (AB) (Fisher Scientific, Ottawa, Canada cat# A643) and centrifuging at 10,000× $g$ for 10–15 min two times. To remove any nucleic acid from the samples 50 μL of benzonase solution (2 mM MgCl2, 100 units benzonase (EMD Millipore/Novagen, St. Louis, MO, USA, cat# 70746-3) in 50 mM HEPES (pH8.3) was added to the filters. They were shaken at 600 rpm for 2 min and incubated for 30 min at room temperature. 100 μL of 50 mM HEPES pH8.3 was then added to the filters and then centrifuged at 10,000× $g$ for 10–15 min. The wash was repeated 2 more times. To digest the proteins in the samples, 50 μL of trypsin solution (1.5 μg of trypsin protease MS Grade) (Pierce, Rockford, IL, USA, cat# 90058) in 50 mM HEPES pH8.3) was added to each filter to the cartridge. The samples were mixed at 600 rpm for 1 min, then incubated overnight at 37 in a humidified chamber. The next day 50 μL of 50 mM HEPES pH 8.3 was added to the filter and it was shaken at 600 rpm for 2 min at room temperature. Next, the filter was inverted into a low bind 1.5 mL Eppendorf tube (Eppendorf, Framingham, MA, USA, cat# 02-681-320) and centrifuged 10,000× $g$ for 3 min to collect the peptides. This was repeated 2 more times. The wash solution containing the tryptic peptides was then concentrated by drying to 1–5 μL using a vacuum centrifuge (speed-vac).Peptides were labeled with TMT six-plex Isobaric Label Reagent Set (Thermo Fisher Scientific, Waltham, MA, USA, cat# 90061) as per the manufacturer's protocol, and labelled samples for each TMT experiment were mixed one-to-one.

## 2.7. Liquid Chromatography and Mass Spectrometry (LC-MS/MS)

Samples were fractionated into 12 fractions by high-pH C18 reversed-phased liquid chromatography using an Agilent 1200 liquid chromatography system (Agilent Technologies, Santa Clara, CA, USA). Each fraction was concentrated to near-dryness using vacuum centrifugation, resuspended in 80 μL of buffer A (2% acetonitrile, 0.1% formic acid) and loaded (2 μL) onto a on a low-pH C18 reversed-phase Easy-Spray column (Thermo Fisher Scientific, Waltham, MA, USA; 50 cm × 100 μm) using an Easy nLC 1000 coupled

to a Q-Exactive Plus mass spectrometer (Thermo Fisher Scientific, Waltham, MA, USA). Peptides were eluted off the column using linear gradients from 5% to 32% buffer B (98% acetonitrile, 0.1% formic acid) over 120 min at a constant flow of 200 nL/min. Total LC-MS/MS run-time per fraction was 160 min.

Two TMT runs were performed on a total of 4 biological replicates for each cell line. The first LC-MS/MS run included biological replicates 1 and 2 of: HPV16 E6 + E7, and HEKn control cells (HEKn transduced with empty lentivectors) and the second LC-MS/MS run included biological replicates 3 and 4. Isobaric tags were shuffled between replicate runs to avoid bias.

### 2.8. Data Analysis

A data-dependent acquisition method was used; dynamically choosing the top 15 abundant precursor ions for fragmentation by HCD. The peptide sequence data was searched against a database containing the SwissProt database (2015_04) restricted to Human (20,216 entries) and HPV (4 entries) using Mascot v2.5 (Matrix Science). Mascot search results were imported into Scaffold Q+ v4.4 (Proteome Software) and filtered using 0.1% FDR for peptides, 1.0% FDR for proteins, and at least two peptides per protein. Median normalization, inter-run and intra-run, peptide spectrum normalization was generated using Scaffold Q+ v4.4.

Further data processing included removing proteins that were not detected in any of the TMT experiments as well as any proteins that were detected in one TMT run but not the other. Principal component analysis was used for data exploration of $\log_2$ protein intensity while a heatmap was generated to evaluate hierarchical clustering of samples [23]. Statistical analyses for differential protein abundance were conducted using the LIMMA (Linear Models for Microarray Data) R package on $\log_2$ normalized protein intensity generated by Scaffold [24]. The *p*-values reported in the manuscript are adjusted by Benjamini-Hochberg (BH) method to correct for multiple hypothesis testing [25]. The threshold for significance was set at an adjusted *p*-value of $\leq$0.02.

To explore the protein interaction networks, biological functions and pathway analyses enriched in our dataset, we employed Ingenuity Pathway analyses (IPA) (QIAGEN Inc., https://www.qiagenbioinformatics.com/products/ingenuitypathway-analysis, accessed on 10 July 2022). STRING v10.5 (Search Tool for the Retrieval of Interacting Genes/Proteins) (accessed 4 August 2022) was used to visualize patterns among the protein networks and biological functions [26].

The IPA analyses were restricted to the 381 proteins significantly upregulated (*p*-value of $\leq$0.02) by at least 1.5-fold (0.6 $\log_2$) change and the 270 proteins significantly downregulated (*p*-value of $\leq$0.02) by at least 1.5-fold (0.6 $\log_2$) change in keratinocytes transduced with HPV16 E6 and E7 lentiviruses compared to the LV-HEKn control keratinocytes.

### 2.9. Immunoblotting

For Western blot analyses, 20 μg of total cellular proteins were added to each well of a 4–20% Mini-PROTEAN® TGX™ Precast Gel (Biorad, Mississauga, Canada cat# 4561093EDU) and electrophoresed at 95 volts for 5 min followed by 200 volts for 30 min. Proteins were transferred to a nitrocellulose membrane using the iBlot2 transfer stacks (Invitrogen, Waltham, MA, USA, cat#IB23001) and Invitrogen's iBlot system. LI-COR TBS Odyssey buffer (LI-COR, Lincoln, NE, USA, cat#927-50100) was used to block the membranes for 1 h at room temperature. An overnight incubation at 4 °C with primary antibodies was followed by a 1-h incubation at room temperature with secondary antibodies. The membranes were imaged on the Odyssey FC imager (LI-COR, Lincoln, NE, USA). Quantification of proteins was performed using Image Studio Lite software from LI-COR. Primary antibodies: p53 (Santa Cruz Biotechnologies sc-126); BST2 (Santa Cruz Biotechnology, Dallas, TX, USA, cat# sc-390719); hTERT (Abcam, Cambridge, UK, cat# ab183105); UCHL1 (Santa Cruz Biotechnology, Dallas, TX, USA, cat#sc-58593); Vinculin (Abcam, Cambridge, UK, cat# ab73412); GAPDH (Invitrogen, Waltham, MA, USA, cat# MA5-15738). Secondary antibodies

included IRDye® 680LT Goat anti-Mouse IgG (LI-COR, Lincoln, NE, USA, cat# 926-68020) and IRDye 800LT Goat anti-Rabbit IgG (LI-COR, Lincoln, NE, USA, cat# 926-32211)

## 3. Results

### 3.1. Lentivirus Transduction

Antibiotic selection verified the successful transduction of keratinocytes. All of the non-transduced control cells were dead within five days of exposure to antibiotics. Subsequently, RT-PCR confirmed the presence of E6 and E7 mRNA in each of the four biological replicates transduced with HPV16 E6 and E7 lentiviruses. Neither E6 nor E7 mRNA were detected in the LV-HEKn biological replicates.

hTERT expression levels were assessed by Western Blot as a measure of immortalization and transformation capacity (Figure 1). Cells expressing both E6 and E7 were maintained in culture and continued to replicate beyond 100 population doublings; actively dividing for more than twice as long as the control cells. The cells expressing HPV16 E6 and E7 were not fully transformed as they did not show evidence of anchorage-independent growth, as determined by plating in soft agar, as previously described [27,28].
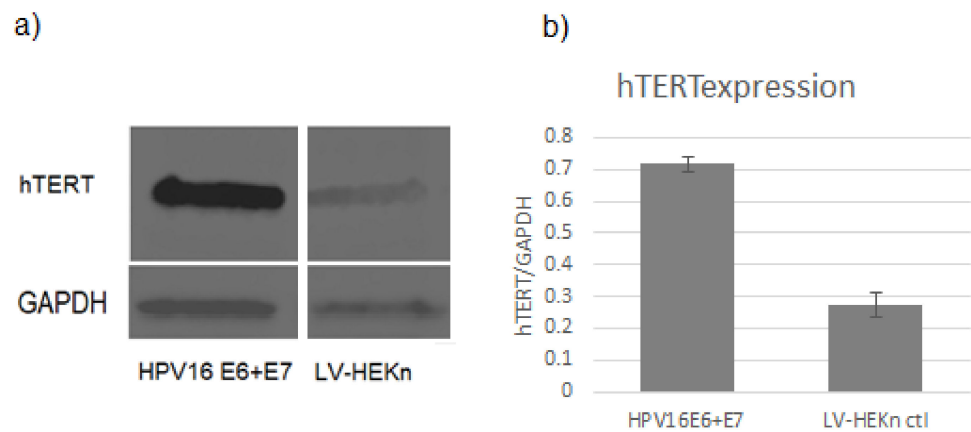


**Figure 1.** (**a**) Western blot experiments showed that hTERT levels were elevated in cells transduced with HPV16 E6 and E7 lentiviruses, compared to control cells (LV-HEKn). (**b**) Bar charts indicate the average level of hTERT normalized to GAPDH for three replicates of each cell line.

### 3.2. Identification of Significantly Differentially Expressed Proteins

The results of the LC-MS/MS analysis revealed 2454 out of 6906 proteins were significantly differentially expressed (adjusted *p*-value $\leq 0.02$) between the cells expressing HPV16 E6 + E7 and the LV-HEKn control cells (Supplementary Table S1). Only the proteins significantly up or downregulated by more than 1.5-fold change were considered in the pathway analyses. There were 381 proteins upregulated by 1.5-fold ($0.6 \log_2$) change and 270 proteins downregulated by $\geq -1.5$-fold ($-0.6 \log_2$) change. The top 10 upregulated and the top 10 downregulated proteins are listed in Tables 1 and 2 respectively.

**Table 1.** List of the top 10 significant proteins most increased in abundance as measured by mass spectrometry-based shotgun proteomics analysis of HEKn cells expressing HPV16 E6 and E7 compared to control cells.

| Protein Name | UNIPROT_ID | Fold Change | Adjusted *p*-Value |
|---|---|---|---|
| Lysosome-associated membrane glycoprotein 3 | LAMP3_HUMAN | 19.6 | $1.17 \times 10^2$ |
| Histone H1.1 | H11_HUMAN | 8.5 | $6.80 \times 10^4$ |
| Bone marrow stromal antigen 2 | BST2_HUMAN | 6.4 | $4.91 \times 10^7$ |
| HLA class I histocompatibility antigen, B-44 alpha chain | 1B44_HUMAN | 5.6 | $3.38 \times 10^7$ |
| Solute carrier family 43 member 3 | S43A3_HUMAN | 5.0 | $3.13 \times 10^4$ |
| Midkine | MK_HUMAN | 4.3 | $1.65 \times 10^3$ |
| Neurofilament heavy polypeptide | NFH_HUMAN | 4.3 | $2.79 \times 10^4$ |
| Histone H1.3 | H13_HUMAN | 4.1 | $1.76 \times 10^2$ |
| Interferon-induced GTP-binding protein Mx2 | MX2_HUMAN | 4.1 | $2.68 \times 10^7$ |
| Tumor necrosis factor ligand superfamily member 10 | TNF10_HUMAN | 4.0 | $3.46 \times 10^6$ |

**Table 2.** List of the top 10 significant proteins most decreased in abundance as measured by mass spectrometry-based shotgun proteomics analysis of HEKn cells expressing HPV16 E6 and E7 compared to control cells.

| Protein Name | UNIPROT_ID | Fold Change | Adjusted *p*-Value |
|---|---|---|---|
| Proline-rich protein 9 | PRR9_HUMAN | −12.8 | $2.14 \times 10^3$ |
| Elafin | ELAF_HUMAN | −8.1 | $1.38 \times 10^3$ |
| Repetin | RPTN_HUMAN | −6.8 | $7.44 \times 10^3$ |
| Keratin, type II cytoskeletal 6B | K2C6B_HUMAN | −6.0 | $7.78 \times 10^4$ |
| Insulin growth factor-like family member 1 | IGFL1_HUMAN | −5.2 | $1.10 \times 10^3$ |
| Small proline-rich protein 3 | SPRR3_HUMAN | −4.5 | $1.80 \times 10^5$ |
| Aldo-keto reductase family 1 member C3 | AK1C3_HUMAN | −4.4 | $3.82 \times 10^4$ |
| Involucrin | INVO_HUMAN | −4.2 | $1.51 \times 10^4$ |
| Filaggrin | FILA_HUMAN | −4.1 | $1.56 \times 10^5$ |
| Alpha-2-macroglobulin-like protein 1 | A2ML1_HUMAN | −4.0 | $5.40 \times 10^4$ |

At 19.6-fold change, LAMP3 was the protein with the most upregulated protein in E6 and E7 expressing cells compared to control ($p = 0.0117$). LAMP3, also known as DC-LAMP, is an integral membrane lysosomal-associated membrane protein whose function is not well defined. LAMP3 may be involved in cell survival during proteasomal inhibition [29,30]. Several proteins related to interferon signaling and immune response were among the top 10 upregulated proteins including, bone marrow stromal antigen 2 (BST2), HLA class I histocompatibility antigen IB-44 alpha chain (IB44), Tumor necrosis factor ligand superfamily member 10 (TNF10) and Interferon-induced GTP-binding protein MX2 (MX2).

Other notable proteins found to be upregulated in the E6 + E7 transduced cells were those associated with DNA replication, including members of the minichromosome maintenance complex (MCM 2-7), Sirtuin-1 (SIRT1) and midkine (MK).

The most downregulated protein was proline rich protein 9 (PRR9) with a −12.8-fold change ($p = 2.14 \times 10^{-03}$). PRR9 is involved in cell organization and differentiation, as are several of the other most substantially downregulated proteins: elafin (ELAF; $p = 1.38 \times 10^{-03}$), repetin (RPTN; $p = 7.44 \times 10^{-03}$), keratin 6B (K2C6B; $p = 7.78 \times 10^{-04}$),

small proline rich protein (SPRR3; $p = 1.80 \times 10^{-05}$), involucrin (INVO; $p = 1.51 \times 10^{-04}$) and filamin (FILA; $p = 1.56 \times 10^{-05}$). Notably, INVO and RPTN were also among the top 20 down regulated proteins in the study by Xu et al. who used TMT-labeled proteomics analysis to determine proteomic dysregulation from cervical squamous cell carcinoma tissue compared to normal cervical tissues [17].

To validate the LC-MS/MS results we measured the amounts of two upregulated proteins in HPV E6 and E7 expressing cells by immunoblotting: Ubiquitin carboxyl-terminal hydrolase isozyme (UCHL1; $p = 5.73 \times 10^{-05}$) and bone marrow stromal antigen 2 (BST2; $p = 4.91 \times 10^{-07}$) were successfully visualized by western blot (Figure 2).
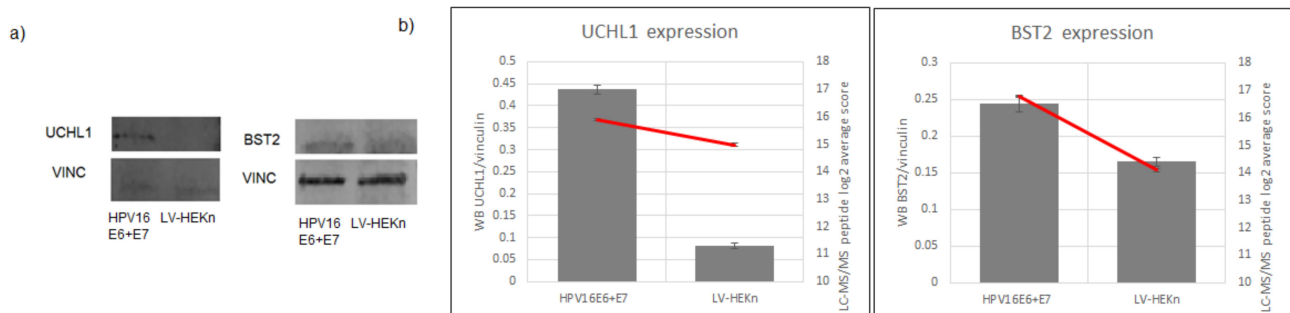


**Figure 2.** Protein levels in HPV16 E6 + E7 cells and LV-HEKn control cells displayed similar trends in Western blots and LC-MS/MS experiments. (**a**) Western blots of UCHL1 and BST2 in HPV16 E6 + E7 cells and LV-HEKn control cells. (**b**) The grey bars represent the abundance of protein measured by Western blot relative to the abundance of load control protein. The red line represents the LC-MS/MS measurements in the two cell lines. Bar charts indicate the average of three replicates of each cell line.

Although p53 was not detected by LC-MS/MS, Western blotting confirmed that p53 was downregulated in cells expressing HPV16 E6 and E7 (Figure 3). It is possible that p53 levels were below the limit of detection of LC-MS/MS because in unstressed cells levels of p53 are restricted by the Mdm2 E3 ubiquitin ligase, while in the presence of high-risk HPV E6 proteins p53 is degraded [31]. Alternatively, it is possible that the absence of p53 in the LC-MS/MS data was due to the limited number of trypsin cleavage sites in p53 that yield usable spectra, or the low abundance of multiple isoforms of p53 [32].
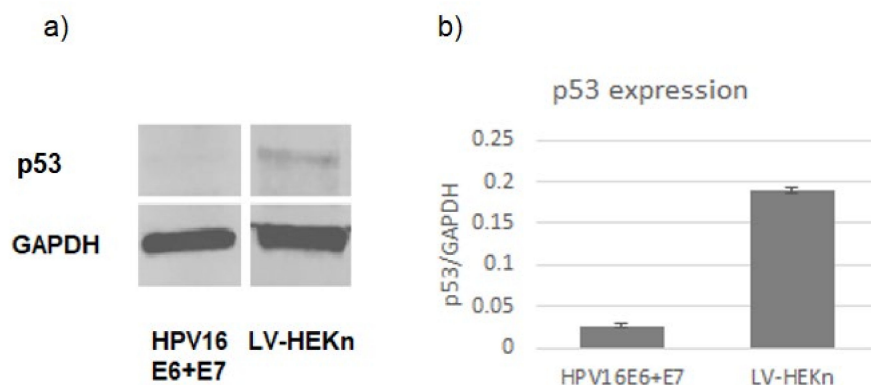


**Figure 3.** (**a**) Western blot experiments showed that p53 levels were reduced in cells transduced with HPV16 E6 and E7 lentiviruses compared to the control cells (LV-HEKn). (**b**) Bar charts indicate the average level of p53 normalized to GAPDH for three replicates of each cell line.

### 3.3. Network Analyses

IPA identified twenty-five networks and putative associated biological functions including Cell Cycle, DNA Replication, Recombination, and Repair, Cell Morphology, Cellu-

lar Movement, Cellular Assembly and Organization; Cell Death and Survival; Antimicrobial Response, Inflammatory Response, Immunological Disease; Cancer; and Dermatological Diseases and Conditions (Table 3).

**Table 3.** Twenty-five protein networks were identified by IPA based on the proteins differentially altered in abundance by $\geq \pm 1.5$-fold change in cells expressing HPV16 E6 and E7 compared to control cells. In addition to up and down regulated molecules, proteins predicted by IPA to participate in a particular network, although not detected by our LC-MS/MS experiments, are also listed. The score reflects the probability of finding the observed proteins in a given network by random chance. A higher score value reflects a lower probability. The top diseases and functions associated with proteins in each network are listed. Multiple networks may have similar biological functions or disease predictions.

| Score | Molecules in Network | | | Top Diseases and Functions |
|---|---|---|---|---|
| | Upregulated | Downregulated | Not Detected | |
| 49 | BTN3A2, BTN3A3, CFAP20, EZH2, FBLN1, HLTF, KIF14, LAMP3, MCM2, MKI67, MUC1, NOLC1, NT5E, PLEKHA4, PSPC1, RBMX, RIF1, UBR7, WBP4 | AMACR, ARL8B, CRCT1, EFNB2, FLG, FTH1, KIF5B, MFAP5, POF1B, RBM3, SLC16A2, SNX18 | Alp, Focal adhesion kinase, GTPase, Secretase gamma | Cancer, Organismal Injury and Abnormalities, Reproductive System Disease |
| 44 | BUD13, CMSS1, EPSTI1, HAT1, NASP, NOP14, PRKRIP1, RBMX2, SLC43A3, TOP1, TRIM22, USP11, VEZF1 | ACAA1, ATP6V0A1, ATP6V1B2, ATP6V1G1, CAMSAP3, CNN2, FAM160A1, HOOK3, KIAA0930, OSBPL9, PDLIM1, SERPINB7, SLC2A6, TRAPPC9, VPS41, VPS8 | AP-3, NFkB (complex), Topoisomerase, Vacuolar H+ ATPase, peptidase, tryptase | Cellular Compromise, Cellular Movement, Hematological System Development and Function |
| 44 | BRIX1, DDX21, DDX27, DDX60L, EBNA1BP2, FTSJ3, H1F0, HIST1H1A, HIST1H1C, HIST1H1E, HMGN2, HNRNPU, IFI16, LYAR, PPM1G, PSIP1, PTMA, RBM28, REXO4, RNF169, RNF213, RRS1, RSL1D1, SURF6, UBTF | HMGCR, MAP2, TNKS1BP1 | PP1 protein complex group, PPAN, phosphatase, Histone H1, Gsk3, P-TEFb, Pp2c | Developmental Disorder, Hereditary Disorder, Infectious Diseases |
| 44 | ARGLU1, CCDC137, CFDP1, DDX49, EXOSC2, EXOSC3, EXOSC5, EXOSC6, EXOSC8, EXOSC9, GLB1L, LAP3, MASTL, MPHOSPH6, SNRNP70, SP140L, SPOUT1, UTP23, ZCCHC8, ZNF740 | APP, C1orf116, CLIC3, CLN5, EOGT, LAD1, RETSAT, SCEL, SH3BGRL3, SPRR4, TOM1L2 | Pi3k class III, Rnr, plasminogen activator, succinate dehydrogenase | RNA Post-Transcriptional Modification, Developmental Disorder, Hereditary Disorder |
| 41 | FBXO6, GINS3, GMPS, GUSB, HIST1H1D, LY75, MCM3, MCM4, MCM5, MCM6, MCM7, NOC3L, NRCAM, ORC3, ORC4, ORC5, SSRP1, TONSL, UHRF1, WARS | DCBLD2, IGSF3, MAN2B1, MAN2B2, MANBA, RNASET2, SGSH, SIAE | E2f, Mannosidase Alpha, Mcm, ORC, RPA, TIP60, Vegf | DNA Replication, Recombination, and Repair, Cell Cycle, Carbohydrate Metabolism |
| 40 | KIF23, KRT19, MCAM, MTHFD2 | DSC1, DSC2, DSG1, DSG3, DSP, EVPL, FLG2, FTL, JUP, KLC3, KRT10, KRT13, KRT15, KRT16, KRT17, KRT23, KRT3, KRT6A, KRT6B, KRT6C, KRT78, KRT80, PKP1 | Alpha catenin, Cytokeratin, Irp, KRT5/6, Keratin, Keratin II, 6,PI3K (complex), PRKAA | Cell Morphology, Embryonic Development, Hair and Skin Development and Function |

Table 3. *Cont.*

| Score | Molecules in Network | | | Top Diseases and Functions |
|---|---|---|---|---|
| | Upregulated | Downregulated | Not Detected | |
| 37 | ANLN, CIT, NUB1, RACGAP1, TLK1 | ARPC3, CALD1, CALML3, CAP1, CORO1A, CORO1B, EEF1B2, ENAH, FAT1, HOMER3, MYH9, MYL12A, MYL6, MYO5A, PLBD2, PLCD1, SLC9A3R1, TPM1, TPM3, TPM4, VAT1 | Actin, Cofilin, Erm, F Actin, G-Actin, Lamin b, Myosin, Pkc(s), Tropomyosin | Cellular Assembly and Organization, Cellular Function and Maintenance, Cellular Movement |
| 36 | ADAR, CBX4, CMPK2, DDX60, IFIT3, MX1, MX2, N4BP1, OASL, PLSCR1, PML, PNPT1,RSAD2, SAMD9L, SMC5, SMC6, SMCHD1, SP110, STAT1, SUMO1, SUMO3, TGM2 | CA12, DHRS1, RPLP1, SPRR1A | IFN Beta, IFN alpha/beta, IL-2R, IL23, Ifn, JAK, JAK1/2, SUMO, cytokine | Antimicrobial Response, Inflammatory Response, Infectious Diseases |
| 31 | APOL2, BRCA2, CYP1B1, DCD, DDX50, ESRRA, GRPEL2, HELZ2, HNRNPC, HNRNPH3, IGFBP4, LGALS3BP, LSM8, NCAPG2, NCAPH2, PRPF19, SMC4, TFAM, TOP2A, TRIM14 | NDUFA4L2, PDLIM5, UBE2E3 | BRCA1-BRCA2-FANCD2-FANCN-RAD51, Collagen type V, Cytochrome bc1, Fanc, LRP, Mitochondrial complex 1, P glycoprotein, PROTEASE, SRC (family) UBE2, cytochrome-c oxidase, snRNP | Cell Cycle, Cellular Assembly and Organization, DNA Replication, Recombination, and Repair |
| 29 | ARID5B, COL1A2, COL6A1, COL6A2, CTSK, MBD3, MMP9, P3H3, P3H4, PDS5B, RCN3, ZNF768 | CAST, CCN1, ITGAV, SDC1, SERPINB13, SERPINB5, SERPINE2, SFRP1, TMBIM1, WNK1 | Cathepsin, Fgf, Fibrinogen, Growth hormone, Integrin, Mi2, Mmp, RNA polymerase I, Smad, TFIIH, Tgf beta, calpain, collagen | Tissue Development, Organismal Injury and Abnormalities, Connective Tissue Development and Function |
| 29 | GBP1, HMGN3, MSLN, MYEF2, NBR1, PLAT, SLC29A1, SRSF9, UNC93B1, ZC3H4 | CPA4, CROT, DPP4, FAP, HTRA1, KLK7, RPS27L, S100A10, SLC20A1, SLPI, SPINK5, TNC, TP53I3 | Collagen type I, Collagen type II, Cpla2, Fc gamma receptor, Fibrin, Kallikrein, P38 MAPK, SYK/ZAP, Serine Protease, Thrombospondin, growth factor, trypsin | Tissue Development, Cell Death and Survival, Cardiovascular Disease |
| 28 | KIF2C, KIF4A, NEFH, NUMA1, SMC1A, SMC2, SMC3, STMN1, UBE2L6 | ACTR1A, AHNAK2, ALDH1A3, CLIP1, DCTN1, DCTN2, DCTN3, DYNC1I2, GM2A, MAPRE3, ROBO1, TUBB2A | Alpha tubulin, BETA TUBULIN, Dynein, Gamma tubulin, MIR101, Mapk, NCK, PDGF-AA, Pak, Pdgf Ab, SMC, Sos, tubulin (family) | Cellular Assembly and Organization, Cellular Function and Maintenance, Tissue Development |
| 28 | BAG2, DNAJC9, HERC5, HNRNPD, HSF1, HSPA2, NSMCE4A, SLC1A5, SPIN1 | BAG3, CRYAB, CSTA, DNAJC5, FILIP1L, HSPB1, MAP1B, PI3, PSTPIP2, SBSN, SEMA3C, TRIAP1, TUBA4A | 26s Proteasome, Calcineurin protein(s), Calmodulin, Complement, HSP, Hdac, Hsp70, Hsp90, MHC Class II (complex), PP2A, Syntaxin, TCF, caspase | Post-Translational Modification, Protein Folding, Cellular Compromise |
| 27 | ANP32B, DHTKD1, EPCAM, FUT8, ICAM1, ISG15, MGME1, RAVER1, RCOR3, TREX1, VRK1 | ACTN1, ACTN4, ASAH1, FABP5, LGALS7/LGALS7B, MVP, PALLD, PDLIM4, PLD1, SLC38A7 | ATPase, Alpha Actinin, Ap2, Casein, Ferritin, GOT, IgG, IgG2a, IgG2b, Igg3, MHC, SCAVENGER receptor CLASS A, hemoglobin, transglutaminase | Cellular Assembly and Organization, Glomerular Injury, Inflammatory Disease |

**Table 3.** *Cont.*

| Score | Molecules in Network | | | Top Diseases and Functions |
|---|---|---|---|---|
| | Upregulated | Downregulated | Not Detected | |
| 27 | ATF1, CHTOP, DCK, ERH, SAMHD1, SRSF4, TRPV2, ZMYND11 | AKAP13, ALS2, APPL1, CALML5, CAMK2G, CDA, DYSF, KIF1C, MAP4, PRKAR2A, RAB5B, SFN, SMPDL3A | 14-3-3, Camk, Cdc2, Cyclin B, Insulin, MAP2K1/2, MTORC2, NFkB (family), Nos, Pde, Pka catalytic subunit, Rab5, Raf, SL1 | DNA Replication, Recombination, and Repair, Nucleic Acid Metabolism, Small Molecule Biochemistry |
| 27 | ACOT4, BRCA1, CDK1, DNMT1, FKBP10, H2AFX, HMGA1, HNRNPR, LMNB1, OGFR, PARP1, PDIA4, PHGDH, TCEA2, TMPO, TTF1 | CSDE1, EPN3, PAM, SDK2, SPRR2D | CD3, Ck2, G protein beta gamma, Histone h3, Holo RNA polymerase II, ITPR, NMDA Receptor, PLC gamma, Pdgfr, Ppp2c, STAT, Sfk, TCR, tubulin | Cellular Assembly and Organization, Cell Death and Survival, Embryonic Development |
| 26 | CGAS, LIG1, NDFIP1, OAS1, OAS2, OAS3, POLD1, POLD2, POLD3, POLE, POLE3, PRIM1, PRIM2, RFC2, WDHD1 | CDH13, GPNMB, MFGE8, PIK3IP1, SCD5, SPRR3 | Akt, Cadherin, Collagen Alpha1,Collagen type VI, DNA Polymerase, DNA polymerase delta, DNA polymerase epsilon, DNA-PK, DNA-directed DNA polymerase, Fascin, Oas, POLbeta-POLepsilon-POLgamma-XRCC1-LIGI-PARP1-PCNA-FEN1, POLbeta-POLgamma-POLepsilon-XRCC1-LIGI-PARP1, nucleotidyltransferase | Cancer, Hematological Disease, Immunological Disease |
| 26 | CD3EAP, CHTF18, DSCC1, FANCI, FEN1, FHL1, IRF2BPL, MDC1, NBN, PCNA, PPHLN1, RBM39, RPA1, RPA2, SUPT16H, TCOF1, TXNIP, UHRF2 | AHNAK, ANK3, DOCK9, KIF13A, LACTB | CaMKII, Cdk, Cyclin A, Fcer1, NADPH oxidase, NFAT (complex), Nfat (family), PI3K (family), PI3K p85, Rac, Rb, TSH | DNA Replication, Recombination, and Repair, Cellular Assembly and Organization, Cellular Function and Maintenance |
| 25 | CSPG4, H1FX, HERC6, MBD4, NES, PMAIP1, TYMP, UCHL1, USP28 | A2ML1, DMKN, FBLIM1, HAS3, ITGB6, LAMP2, MICALL2, SLC25A20, TRIM29, VPS29, VPS35 | Collagen type III, Collagen type IV, Collagen(s), Complement component 1, DUB, ERK, Filamin, GPIIB-IIIA, Laminin (complex), Laminin1,RAB7, S100, chymotrypsin, elastase, gelatinase | Hereditary Disorder, Neurological Disease, Organismal Injury and Abnormalities |
| 25 | BAZ1B, CBX1, CBX3, CBX5, CHAF1A, CHAF1B, DSN1, HP1BP3, LBR, MIS12, MSH6, NT5C3A, PMF1/PMF1-BGLAP, RFC1, RFC4, RFC5, SP100 | EXOC7,SLC1A3,SPRR1B | BRCA1 complex B, Basc, CAF-1Fgfr, H-2db, HP1, Hspg, L-type Calcium Channel, Ldh (complex), MRN, MutS alpha, PCNA-CAF1, Pde4, Pka, Rfc | Cellular Development, Cellular Growth and Proliferation, Embryonic Development |

**Table 3.** *Cont.*

| Score | Molecules in Network | | | Top Diseases and Functions |
|---|---|---|---|---|
| | Upregulated | Downregulated | Not Detected | |
| 23 | CFB, DDX58, DTX3L, EIF2AK2, IFI35, IFIT1, MACROD1, MLH1, NMI, PARP12, PARP14, PARP2, PARP9, RNF114, TDRD7, TNFAIP3, TNFSF10 | NPC2, TPRG1L | ATM/ATR, H2AF, Hsp27, I kappa b kinase, IFI35, Ikb, Ikk (family), Inflammasome (Nalp3, Asc, Casp1), MLH1-MSH2-MSH6-PMS2, PARP, Ras homolog, Tlr, Tnf (family), Tnf receptor, cytochrome C, mismatch repair, pentosyltransferase | Connective Tissue Disorders, Immunological Disease, Inflammatory Disease |
| 23 | ASNS, CCPG1, DHRS13, DHX40, FANCD2, HLA-A, INA, RBCK1, RNPS1, SIRT1, SPAG7, SUZ12, TNIP1 | DMKN, EEF1G, GAN, RPTN, S100A8, YWHAG | CNTN6, Csprs (includes others), EGLN, H2-Q8, MTORC1, MYCT1, NSMF, Nc2, PRSS27, RAB20, RNA polymerase II, SMTNL2, Sod, TNIP1, Ubiquitin, VWA3B, chemokine | Connective Tissue Disorders, Dermatological Diseases and Conditions, Immunological Disease |
| 21 | B2M, BST2, ERAP1, HLA-B, HLA-C, HLA-E, HLA-F, HLA-G, H, MAT2B, PSMB10, PSMB9, PSME1, PSME2, TAP1, TAP2, TAPBP, TAX1BP1 | SERPINB3 | 20s proteasome, ERK1/2, HLA Class I, HLA-B27, Hla-abc, Ifnar, Immunoproteasome Pa28/20s, KIR, MAP1LC3, MHC (Major Histocompatibility Complex), MHC CLASS I (family), MHC Class I (complex), MHC I-$\alpha$, PKC alpha/beta, Stat1-Stat2, Tap, peptide-Tap1-Tap2 | Antigen Presentation, Protein Synthesis, Cellular Function and Maintenance |
| 17 | ANP32E, CIR1, FKBP10, LIN54, MELTF, SLC25A35, SMOC1, VPS72 | CYB5R1, DSC2, LAD1, MEGF9, SERF2, ZNF185 | C11orf52, DENND5B, Dynamin, ESR2, GABPB2, HIF1AN, HNF4A, L2HGDH, MMP17, NUPR1, OSER1, PHTF1, SMOC1, SPIRE1, THAP4, TMEM50B, TMEM53, TNF, TRIM25, TSNAXIP1, UTP11 | Tissue Development, Cell Morphology, Cellular Compromise |
| 17 | ANP32B, FBLN1, HLA-B, MCAM, NRCAM | ANO10, CAP1, CLCA2, CNN2, GLTP, HTRA1, KCNK6, MPV17L2, SEMA3C, SNX30 | AQP3, CD99,C EMIP2, EMG1, ESR1, FN1, HYAL1, KHDRBS1, MYLK2, NDC1, NUP88, OSTF1, RPS3, SLC26A2, SLC44A1, TCF/LEF, TCF7L2, TNS3, TWIST, UGT8 | Cellular Movement, Hematological System Development and Function, Immune Cell Trafficking |

The biological function gene ontology (GO) terms assigned to our data using STRING software, corroborated many of the biological functions identified by IPA analyses (Figures 4–6). Proteins which were either up or downregulated by $\geq\pm1.5$-fold change in keratinocytes transduced with HPV16 E6 and E7 were included in the analysis.
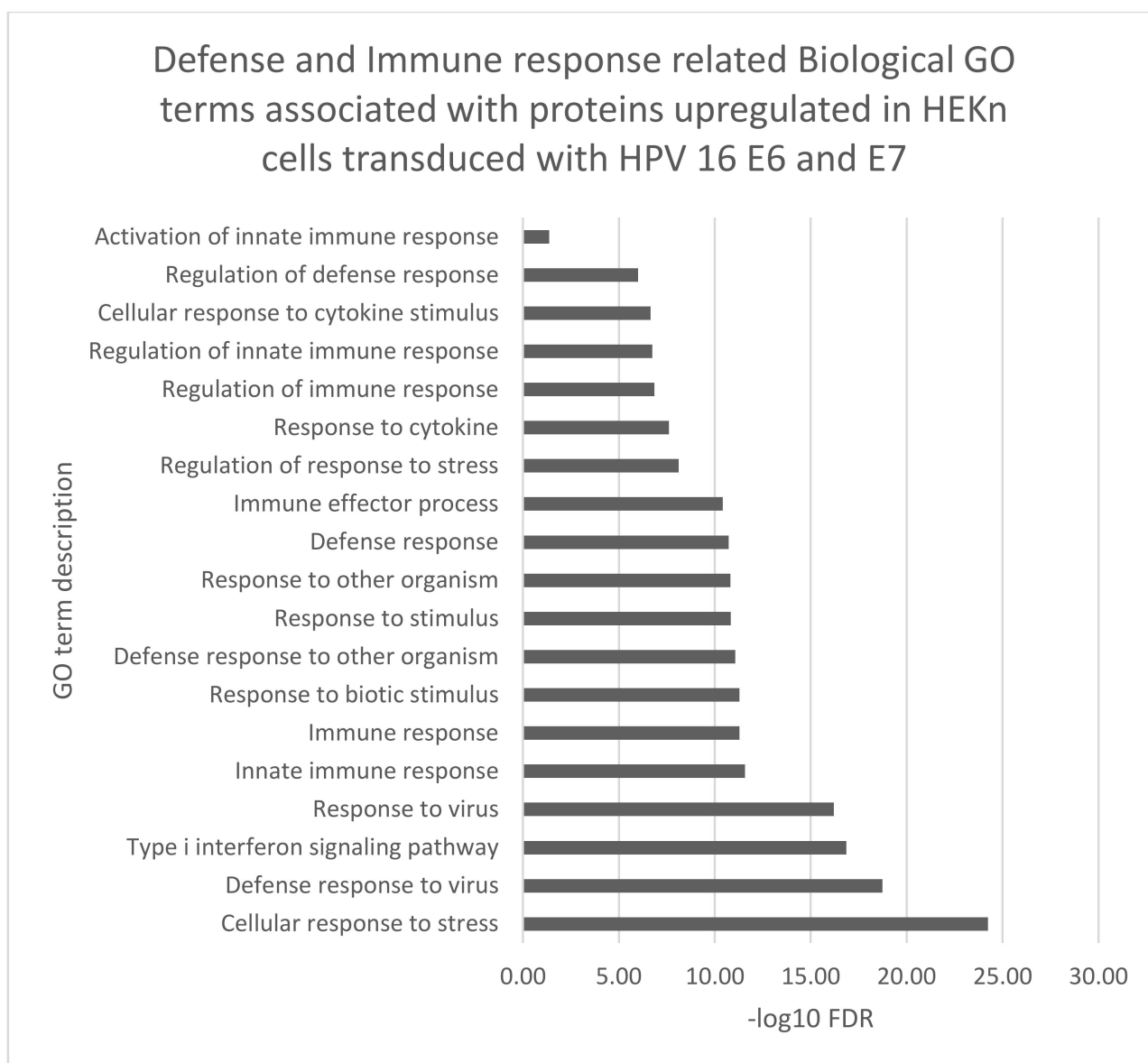
**Figure 4.** Biological GO terms related to defense immune responses were associated with the proteins with significantly increased expression (adjusted *p*-value $\leq 0.02$) by $\geq\pm1.5$-fold change in keratinocytes transduced with HPV16 E6 and E7. FDR (False discovery rate).

Several Biological GO terms associated with the proteins with significantly increased expression were related to immune response interferon response and inflammation. Proteins, such as 2′-5′-oligoadenylate synthase 1 (OAS1), signal transducer and activator of transcription 1 (STAT1) and E3 ISG15-protein ligase (HERC5) contributed to these GO term predictions.

DNA damage and apoptosis were predicted to be associated with proteins whose expression was significantly increased (adjusted *p*-value $\leq 0.02$) by $\geq\pm1.5$-fold change in keratinocytes transduced with HPV16 E6 and E7 (Figure 4). Breast cancer type 1 susceptibility protein (BRCA1), DNA topoisomerase 2-alpha (TOP2A) and several histones (H1X, H10 H11, H12, H13) were among the proteins with significantly increased expression in our data. These proteins are predicted to influence apoptosis and DNA damage responses.
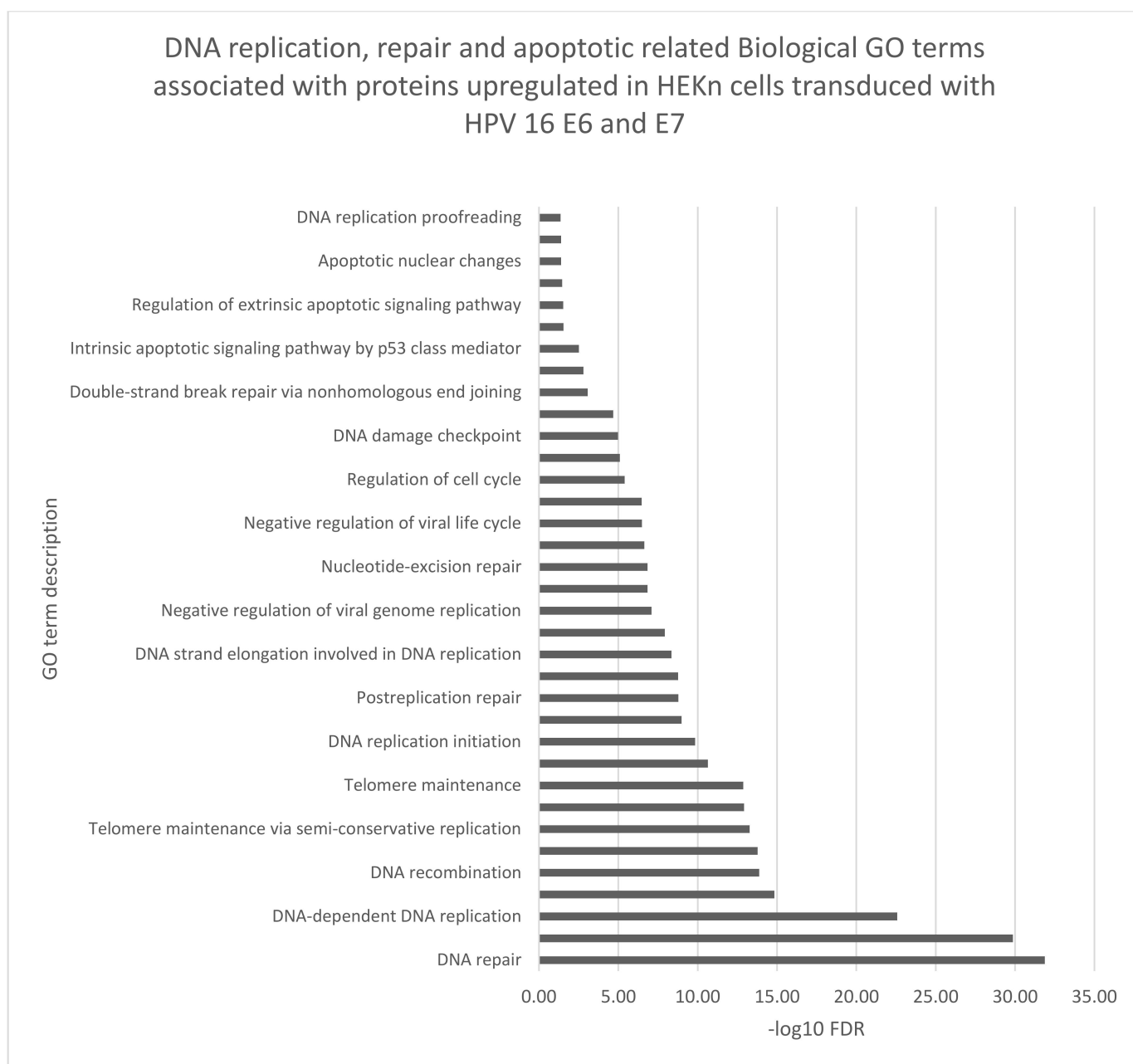
**Figure 5.** Biological GO terms related to DNA damage and apoptosis were associated with the proteins with significantly increased expression (adjusted *p*-value ≤ 0.02) by ≥±1.5-fold change in keratinocytes transduced with HPV16 E6 and E7. FDR (False discovery rate).

Finally, thirty-two biological GO terms associated with epidermal differentiation, keratinization and cytoskeletal organization were associated the proteins with significantly reduced expression (Figure 6). This group of significantly downregulated proteins includes several keratins, small proline rich proteins (SPR1A, SPR1B, SPRR2D, SPRR3, and SPRR4), desmocollins (DSC1, DSC2) which may influence the epidermal differentiation.
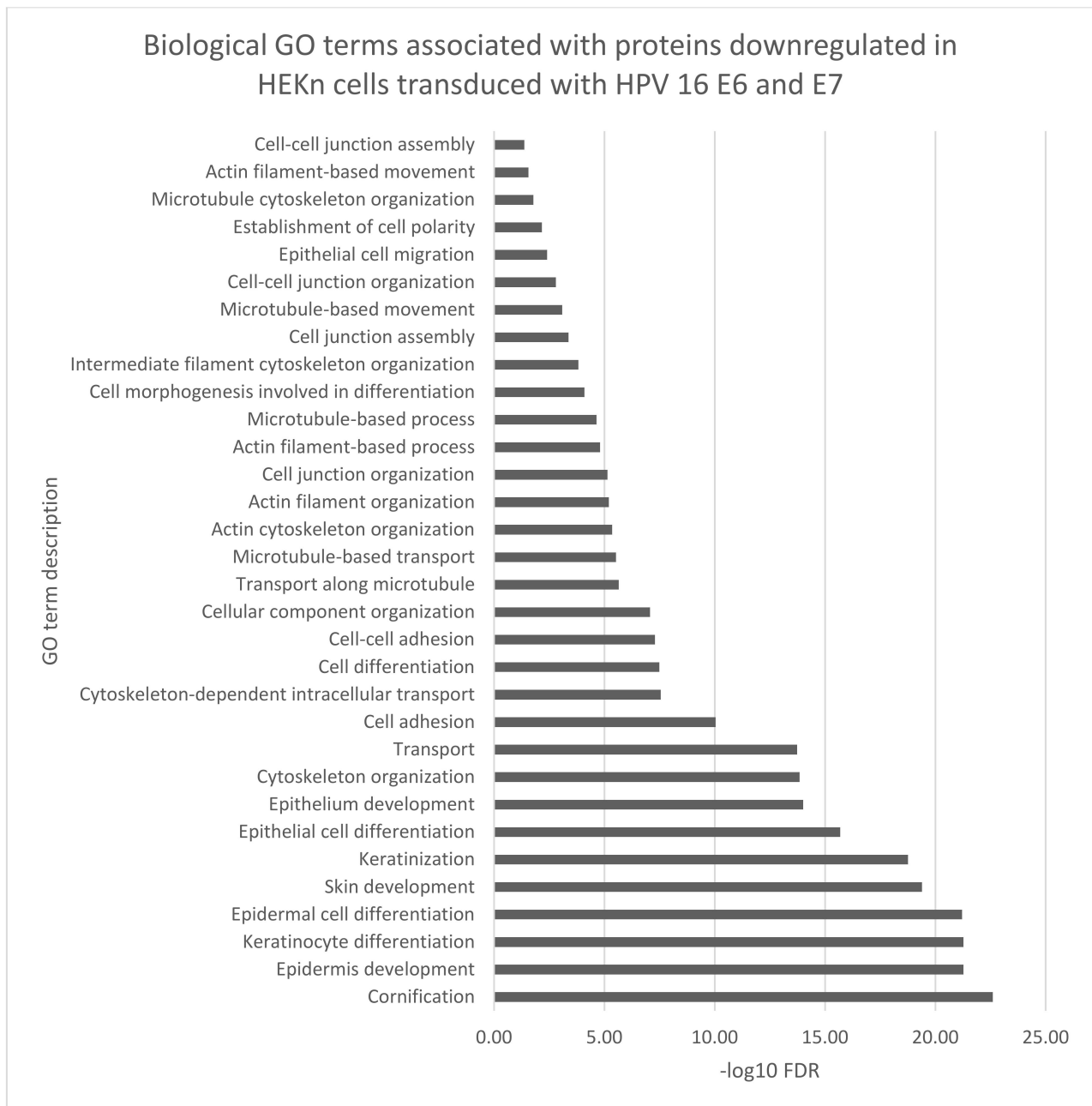
## Biological GO terms associated with proteins downregulated in HEKn cells transduced with HPV 16 E6 and E7



**Figure 6.** Thirty two- biological GO terms associated with epidermal differentiation, adhesion and cytoskeletal organization were predicted to be related to proteins with a reduced expression by $\geq \pm 1.5$-fold change (adjusted *p*-value $\leq 0.02$) in keratinocytes transduced with HPV16 E6 and E7 FDR (False discovery rate).

### 3.4. Canonical Pathway Analyses

IPA identified fifty-five canonical pathways predicted to be affected by the proteins significantly differentially expressed in HEKn cells transduced with HPV16 E6 and E7 (Figure 7). Understanding which pathways are affected by HPV oncoproteins may elucidate key host processes that are modulated by E6 and E7. We discovered that many of the altered canonical pathways were related to Cell cycle control, replication, Damage response, Antigen presentation pathway, Interferon signaling and apoptotic signaling.
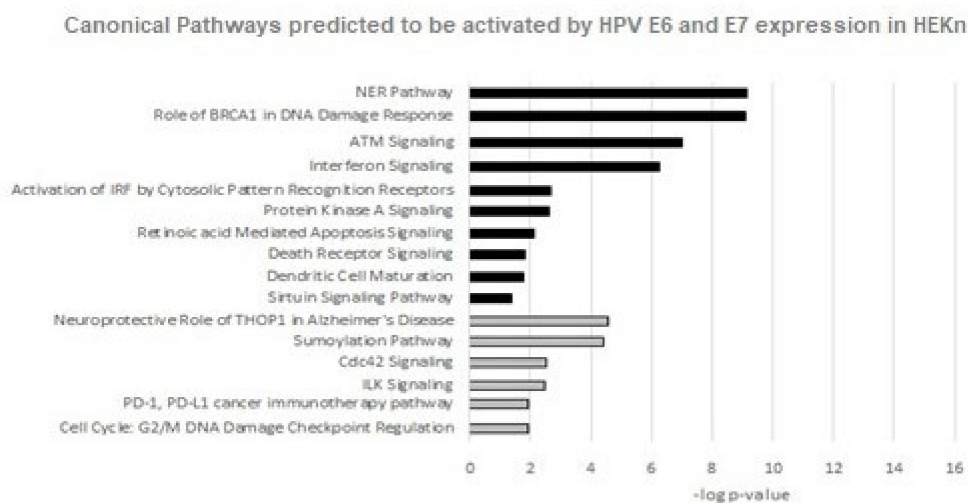
**Figure 7.** Canonical pathways predicted to be affected in HEKn cells expressing HPV16 E6 and E7 oncoproteins. Included in this analysis were proteins significantly differentially expressed (adjusted *p*-value $\leq$ 0.02) by $\geq \pm 1.5$-fold change. Black shading indicates a predicted increase in activity and grey shading indicates a predicted inhibition of canonical pathway, based on current evidence in the Qiagen Ingenuity Pathway database.

For six of these pathways IPA predicted decreased activity: CDC42 signaling, Sumoylation Pathway, Cell Cycle: G2/M DNA Damage Checkpoint Regulation, Neuroprotective Role of THOP1 in Alzheimer's Disease, PD-1,PD-L1 cancer immunotherapy pathway and ILK Signaling.

Similarly, there was enough evidence for IPA to predict the activation of ten canonical pathways: The Role of BRCA1 in Damage response, NER pathway, ATM signaling, Interferon signaling, Retinoic mediated apoptosis signaling, Activation of IRF by Cytosolic Pattern Recognition Receptors, Protein Kinase A Signaling, Death receptor signaling, Sirtuin Signaling pathway and Dendritic Cell Maturation.

The activation or inhibition of the other canonical pathways could not be predicted based on the current data in the IPA ingenuity database, but included pathways related to DNA damage, antiviral responses, cell survival and proliferation.

## 4. Discussion

### 4.1. Altered Protein Abundance in HEKn Expressing HPV16 E6 and E7

Persistent infection with high-risk HPV types is strongly associated with cancer. Although the mechanisms leading to transformation are not entirely elucidated, the persistent expression of E6 and E7 proteins of high-risk HPV types are known to actuate cell transformation [5,33–36]. Increased understanding of the proteins and pathways altered by the E6 and E7 oncoproteins should elucidate the mechanisms of viral persistence and the immune evasion tactics employed by HPV16 E6 and E7 preceding transformation. Of particular interest are the proteins or pathways that could be of therapeutic or prognostic value.

To determine the effects of the E6 and E7 oncoproteins on the host proteome, we performed LC shotgun proteomics analysis using HEKn transduced with lentiviruses containing HPV16 E6 and E7. One of this limitations of our study is that we did not verify the expression of the E6 and E7 by Western blot, however we did confirmed the presence of E6 and E7 mRNA by RT-PCR. Notably the cells expressing E6 and E7 were not transformed as demonstrated by soft agar assays, but did show altered expression of p53 and hTert. Interestingly, p16/CDKN2A, a cytological marker of transformation in HPV-induced cervical high-grade dysplasia, was not regulated in the presence of E6 and E7.

We elected to use a 2D HEKn culture model for this project because, despite its simplicity, it is appropriate for the investigation into effects of the viral proteins on the keratinocyte proteome. In vitro organotypic 3-D culture models are better suited for investigations into the HPV life cycle [37].

Our proteomic analysis identified 2454 significantly differentially expressed proteins (adjusted *p*-value $\leq$ 0.02). The subsequent pathway analyses were restricted to proteins significantly differentially expressed by $\geq$+1.5-fold change or $\leq$−1.5-fold change, which yielded a data set of 651 proteins which were subjected to pathway and network analyses.

There were a few recurring themes observed in our data, many of the upregulated proteins and their associated pathways were related to innate immune responses, interferon signaling and inflammation, as well as DNA replication, DNA damage response, cell proliferation, and cell death and survival. Among the downregulated proteins were those involved in epidermal differentiation.

### 4.2. HPV16 E6 and E7 Affect DNA Replication and DNA Damage Response Pathways

HPV must appropriate the host DNA replication machinery to amplify their viral genome. Although the HPV proteins E1 and E2 form the actual viral replication complex, the E6 and E7 oncoproteins have an essential, albeit indirect, role in viral replication. The binding of the tumor suppressor pRb by E7 allows the E2F transcription factor to activate DNA replication and there is increasing evidence that HPV also manipulates the DNA damage response pathways as part of its replication strategy [38]. The effects of HPV16 E6 and E7 on DNA replication and DNA damage responses are supported by our data, as several proteins and canonical pathways related to activation of DNA replication and DNA damage responses were found to be deregulated in HEKn expressing HPV16 E6 and E7 proteins.

Mini-Chromosome Maintenance proteins (MCM), make up an essential component of the DNA pre-replication complex. As part of that complex, six MCM proteins (MCM2–MCM7) form a hexamer which together with cell division cycle 6 (CDC6) and Chromatin Licensing And DNA Replication Factor 1 (CDT1) binds to a DNA origin of replication and initiates DNA replication [39]. Typically, levels of MCM proteins are only increased during the S-phase of the cell cycle. MCM proteins are strongly associated with cell proliferation and their deregulation has been recognized as significant prognostic biomarkers for several types of cancer, including cervical cancer [40–42]. In our data, MCM2-7 were all upregulated in the HEKn cells expressing HPV16 E6 and E7 in agreement with a previous study which documented the upregulation of MCM2-7 mRNA in cervical cancer and precancerous lesions [41]. The mechanisms responsible for the elevated levels of MCM in cervical cancers are not well described, but in lung cancer, YAP/TAZ expression has been cited for promoting the upregulation of MCM7 transcription leading to cell proliferation [43]. YAP and TAZ proteins are key regulators of HIPPO signaling pathway, but neither of these proteins, nor the HIPPO signaling pathway, was found to be significantly differentially altered in IPA analyses between HPV16 E6 and E7 expressing HEKn cells and control cells. It is likely that in the cells expressing HPV16 E6 and E7, the increase in MCM proteins is related to the repression of pRb by E7 because pRb loss or repression is known to permit cyclin E1, a target of pRb, to recruit MCM proteins to pre-replication complexes [44].

Ataxia-telangiectasia mutated (ATM) signaling and DNA Double-Strand Break Repair by Homologous Recombination were among the canonical pathways predicted to be significantly affected in the cells expressing HPV E6 and E7. Typically, when the DNA of a cell is damaged, one of the cellular DNA damage response pathways, ATM or ataxia-telangiectasia mutated Rad3-Related (ATR), becomes activated arresting the cell cycle until the damaged is repaired. Intriguingly, it appears that HPV replication promotes the activation of DNA damage repair signaling and HPV is not unique in this approach to viral DNA replication. The polyomavirus simian virus 40 (SV-40) and several herpesviruses also activate the ATM and recruit DNA repair factors for viral replication [45–47]. Interestingly,

using LC-MS/MS, Guzel et al. also recently reported that DNA repair pathways were altered in early stages of cervical cancer [14].

Two members of the ATM pathway significantly upregulated in our data associated with HPV16 E6 and E7 expression include Breast cancer type 1 susceptibility protein (BRCA1) (+2.8-fold $p$ = 0.0071) and the histone H2AX (+1.8-fold $p$ = 0.024).

Upon detection of DNA damage, the histone H2Ax locates to the site of damage and is phosphorylated by ATM to γ-H2AX. Together with other members of the DNA damage response, BRCA1 and γ-H2AX activate cell cycles checkpoints to arrest the cell cycle and initiate homologous recombination or non-homologous end-joining DNA repair. Being a tumor suppressor, it is interesting that HPV E6 and E7 would promote BRCA1 expression, but remarkably, these viral oncoproteins have evolved a mechanism to bind and functionally inactivate BRCA1 although they do not proteolytically degrade it [48]. Via their zinc finger domains, E6 and E7 prevent BRCA1 from repressing the estrogen-receptor-α (ER-α) transcriptional activity and prevent the inhibition of cMyc transactivation by BRCA1 [48].

*4.3. Immune Evasion and Interferon Signaling Aberration by HPV16 E6 and E7*

Modification of protein acetylation is one mechanism by which HPV is known to evade the host's immune system and promote viral DNA replication [49–51]. Here we have proteomic evidence documenting the differential levels of protein deacetylases related to HPV16 E6 and E7 expression. Among the upregulated proteins from HEKn cells expressing HPV16 E6 and E7, there were three protein deacetylases, HDAC2 and HDAC7, and sirtuin (SIRT1) which were upregulated by 1.4, 1.5, and 1.7-fold change respectively. Histone deacetylases (HDAC) and SIRT1 deacetylases, also known as NAD-dependent deacetylase sirtuin-1 have previously been shown to be deregulated in cancers, including HPV associated cancers [49,50,52–54]. Interestingly, elevated levels of HDAC and SIRT1 have been linked to HPV immune evasion strategies. For example, HPV E7 reduces TLR9 expression by recruiting HDAC2 to the TLR9 regulatory region, ultimately repressing interferon responses [51]. Although there is recent evidence that SIRT1 represses the AIM2 (absent in melanoma inflammasome) innate immune response to infection by DNA viruses, promoting survival and proliferation of HPV positive cells, there is no evidence of the downregulation of AIM2 associated proteins such as interleukin-1β or caspase among our list of significantly differentiated proteins [54]. SIRT1 can target p53 for deacetylation, which would presumably enhance the abrogation of the p53 pro-apoptotic signaling pathway promoted by HPV E6.

In addition to immune evasion, SIRT1 is required for HPV viral replication. SIRT1 forms a complex with HPV E1 and E2 proteins at the HPV origin of replication, deacetylates E2 and recruits the DNA repair protein Werner helicase [38,49,55]. Fittingly, Werner helicase interacting protein 1 was observed in our data to be upregulated in HEKn cells expressing E6 and E7.

The fidelity of HPV replication also relies on SIRT1. Knockdown of SIRT1 in HPV16 infected cells results in a highly mutated genome due to the failure to recruit to the E1/E2 complex [49,55]. Furthermore, SIRT1 knockdown in HPV31 infected cells diminishes the number of viral genomes in the host cells [50].

Interferon signaling and antiviral responses were among the biological functions and canonical pathways, which IPA predicted to be altered in HEKn cells expressing HPV16 E6 and E7. Production of type 1 Interferon results from the detection of viral DNA by host pattern recognition receptors and the initiation of the innate immune signaling. One of the proteins that likely contributed to the activation of interferon signaling and antiviral responses predicted for our data is LAMP3. Previous studies have associated LAMP3 with increased levels of interferon-dependent anti-viral genes [56].

Our findings agree with a previous study, where LAMP3 mRNA was found to be highly expressed in 100% of cervical cancers [57]. LAMP3 overexpression is highly associated with metastatic potential and it has been proposed that LAMP3 may be an important

prognostic biomarker for cervical cancer [57]. In addition, high levels of LAMP3 have been identified as prognostic biomarkers in esophageal squamous cell carcinoma, hepatic and ovarian cancers [58–60].

LAMP3, also known as DC-LAMP, is an integral membrane lysosomal-associated membrane protein whose role is not well defined. There is some evidence that LAMP3 is required for cell survival during proteasomal inhibition and there have been some recent investigations into the role of LAMP3 in different cancers [29,30]. For example, in *osteosarcoma cells*, *LAMP3* significantly increased cell viability and abrogated apoptosis by regulating *p53* expression [30]. The role of LAMP3 has also been explored in HPV positive cells. In HeLa cells, LAMP3 is associated with increased levels of interferon-dependent anti-viral genes: STAT-1, IRF7, HERC5, ISG20 and OAS1; silencing of LAMP3 results in their downregulation [56]. Fittingly, in our data STAT-1, HERC-5 and OAS1 were upregulated in the cells expressing HPV16 E6 and E7 proteins.

Another significantly upregulated protein linked to interferon expression in cells expressing HPV16 E6 and E7 is Bone Marrow Stromal Cell Antigen (BST2). While BST2 is induced by interferon, it also negatively regulates interferon by binding with the Immunoglobulin-like transcript 7 in plasmacytoid dendritic cells [61,62]. The ability to modulate interferon levels would presumably limit the negative consequences of protracted interferon exposure on the host.

An increase in BST2 has been reported in several types of cancer including cervical cancer [63–68]. The overexpression of BST2 in breast cancer cells is associated with enhanced cell proliferation and inhibition of apoptosis [69]. BST2 enhances survival through proteasome-mediated degradation of the proapoptotic protein BIM (Bcl-2 like protein 11), a member of the Bcl-2 family. Mahauad-Fernandez and Okeoma recently described a mechanism by which BST2 dimerization activates ERK1/2 and phosphorylates and degrades BIM, preventing anoikis in breast cancer cells [70]. BIM was not significantly differentially expressed in our data however.

HPV16 E6 can bind the interferon regulatory factors, IRF3 and IRF9, to thwart interferon signaling [71]. Although we did not find IRF3 or IRF9 to be differentially expressed, we did observe that UCHL1 (Ubiquitin carboxy-terminal hydrolase L1), a protein known to affect IRF3 phosphorylation, was upregulated by 1.9-fold change in HEKn cells expressing HPV16 E6 and E7 [72]. UCHL1 is a deubiquitinating enzyme that prevents the polyubiquitination of tumor necrosis factor 3 (TRAF3) and also results in the degradation of NEMO, a modulator of NFkB (nuclear factor kappa-light-chain-enhancer of activated B cells) signaling [72]. NFkB signaling regulates cytokine production and cell survival signaling, and its dysregulation has long been correlated to cancers [73].

Midkine, a heparin-binding cytokine that promotes cell proliferation and migration, was among the top 10 most upregulated proteins in HEKn cells expressing HPV16 E6 and E7. Midkine has previously been reported to be upregulated in cervical, bladder, esophageal and gastric cancers and increased levels of midkine are associated with poor prognosis [74–77]. A previous study explored midkine's effects on growth and survival. That group added midkine to the medium of cultured neuronal cells and found that this resulted in activated MAPK and PI3K signaling, while caspase-3 was inhibited [78]. It was subsequently discovered that midkine promotes cell proliferation and survival by phosphorylating the ALK (anaplastic lymphoma receptor kinase) in fibroblasts leading to MAPK and PI3K activation [79]. Activation of MAPK and PI3K does not fit with our data however as MAPK is predicted to be strongly inhibited in our cells expressing HPV16 E6 and E7. The implications of midkine upregulation in HEKn cells expressing HPV16 E6 and E7 remains to be explored and may be worth pursuing, as midkine has garnered attention as a therapeutic target for one type of lung cancer [80].

### 4.4. Dysregulation of the Keratinized Barrier by HPV16 E6 and E7 Expression

The third biological trend highlighted in our proteomic analyses was dysregulation of epidermal differentiation and the inhibition of the formation of the keratinized barrier.

These biological functions were predicted to be significantly downregulated in HEKn cells expressing HPV16 E6 and E7. Seven of the top ten downregulated proteins in the HPV16 E6 and E7 cell line were associated with epidermal differentiation: Proline-rich protein 9, elafin, repetin, keratin type II, small proline-rich protein 3, involucrin and filaggrin. Interestingly, a previous gene expression study also found several genes associated with keratinocyte differentiation to be downregulated in keratinocytes expressing high-risk E6 proteins [81]. In that study, genes encoding elafin, small proline-rich proteins, keratins and involucrin were among the differentiation-associated genes significantly affected [81].

The keratinized layer of the epithelium acts as a mechanical and permeability barrier, and so its inhibition by HPV might be essential to foster the egress of viral particles from the host. Co-incidentally, the inhibition of differentiation is a hallmark of cell transformation. Normally, primary keratinocytes undergo an irreversible differentiation process forming a keratinized envelope when deprived of anchorage to a semi-solid medium [82]. Malignant cells, on the other hand, fail to differentiate and do not form a keratinized envelope when cultured in an anchorage-independent manner [82]. Despite the downregulation of the proteins associated with epidermal differentiation in our cells, when grown on soft agar there was no evidence of colony formation.

## 5. Conclusions

Using LCTMT-labelling and shotgun proteomics with pathway analysis we have catalogued proteomic signatures significantly differentially expressed in HEKn cells expressing HPV16 E6 and E7 proteins. Our data support previous gene expression studies linking HPV to the manipulation of the host's DNA damage response pathways, DNA replication and interferon signaling. We have shown that several DNA damage response proteins and interferon modulating proteins including BRCA1, H2AX, SIRT1 and LAMP3 are unambiguously upregulated in primary keratinocytes expressing HPV16 E6 and E7 oncoproteins. Our study also identified proteins, such as the heparin-binding protein midkine and the ubiquitinase UCHL1, to be upregulated. These proteins warrant further exploration regarding their relationship with HPV infection.

Notably, some of these significantly differentially up-regulated proteins have potential as biomarkers or for the development of therapies. For example, LAMP3, which was the most upregulated protein in the HEKn cells transduced with HPV16 E6 and E7, is regarded as a biomarker of several cancers [58–60]. Further investigation into LAMP3 expression in various stages of cancers is needed to determine the prognostic value of this protein. Midkine is also interesting as a possible therapeutic target; not only is midkine considered a prognostic indicator for various cancers, but it has also garnered attention as a therapeutic target. An inhibitor of midkine has recently been described as a potential mesothelioma treatment [80].

Future studies could include validating the clinical implications of these findings in vivo using CIN lesions or determining if any of these differentially expressed proteins or deregulated pathways may be useful as therapeutic targets in HPV related cancers or for the identification of biomarkers for HPV prognosis. Although there are vaccines targeting several of the high-risk types of HPV, there are millions of people persistently infected with HPV. For these people, non-surgical therapeutic options are lacking. Further characterization of the proteins or pathways identified in this study will advance our understanding of the mechanisms of HPV16 E6 and E7 mediated immortalization and transformation of keratinocytes.

## References

1. zur Hausen, H. Papillomaviruses and cancer: From basic studies to clinical application. *Nat. Rev. Cancer* **2002**, *2*, 342–350. [CrossRef]
2. Francki, R.; Fauquet, C.; Knudson, D.; Brown, F. Virology Division of the International Union of Microbiological Societiesl. In *Classification and Nomenclature of Viruses: Fifth Report of the International Committee on Taxonomy of Viruses*; Springer: Berlin/Heidelberg, Germany, 2012.
3. Small, W., Jr.; Bacon, M.A.; Bajaj, A.; Chuang, L.T.; Fisher, B.J.; Harkenrider, M.M.; Jhingran, A.; Kitchener, H.C.; Mileshkin, L.R.; Viswanathan, A.N. Cervical cancer: A global health crisis. *Cancer* **2017**, *123*, 2404–2412. [CrossRef] [PubMed]
4. Hawley-Nelson, P.; Vousden, K.H.; Hubbert, N.L.; Lowy, D.R.; Schiller, J.T. HPV16 E6 and E7 proteins cooperate to immortalize human foreskin keratinocytes. *EMBO J.* **1989**, *8*, 3905–3910. [CrossRef] [PubMed]
5. Münger, K.; Phelps, W.; Bubb, V.; Howley, P.; Schlegel, R. The E6 and E7 genes of the human papillomavirus type 16 together are necessary and sufficient for transformation of primary human keratinocytes. *J. Virol.* **1989**, *63*, 4417–4421. [CrossRef] [PubMed]
6. Thomas, M.; Pim, D.; Banks, L. The role of the E6-p53 interaction in the molecular pathogenesis of HPV. *Oncogene* **1999**, *18*, 7690. [CrossRef]
7. Boyer, S.N.; Wazer, D.E.; Band, V. E7 protein of human papilloma virus-16 induces degradation of retinoblastoma protein through the ubiquitin-proteasome pathway. *Cancer Res.* **1996**, *56*, 4620–4624.
8. Liu, Y.; Chen, J.J.; Gao, Q.; Dalal, S.; Hong, Y.; Mansur, C.P.; Band, V.; Androphy, E.J. Multiple functions of human papillomavirus type 16 E6 contribute to the immortalization of mammary epithelial cells. *J. Virol.* **1999**, *73*, 7297–7307. [CrossRef]
9. Hu, D.; Zhou, J.; Wang, F.; Shi, H.; Li, Y.; Li, B. HPV-16 E6/E7 promotes cell migration and invasion in cervical cancer via regulating cadherin switch in vitro and in vivo. *Arch. Gynecol. Obs.* **2015**, *292*, 1345–1354. [CrossRef]
10. White, E.A.; Kramer, R.E.; Tan, M.J.; Hayes, S.D.; Harper, J.W.; Howley, P.M. Comprehensive analysis of host cellular interactions with human papillomavirus E6 proteins identifies new E6 binding partners and reflects viral diversity. *J. Virol.* **2012**, *86*, 13174–13186. [CrossRef]
11. White, E.A.; Sowa, M.E.; Tan, M.J.A.; Jeudy, S.; Hayes, S.D.; Santha, S.; Münger, K.; Harper, J.W.; Howley, P.M. Systematic identification of interactions between host cell proteins and E7 oncoproteins from diverse human papillomaviruses. *Proc. Natl. Acad. Sci. USA* **2012**, *109*, E260–E267. [CrossRef]
12. Thatte, J.; Massimi, P.; Thomas, M.; Boon, S.S.; Banks, L. The HPV E6 PDZ Binding Motif links DNA Damage Response Signaling to E6 Inhibition of p53 Transcriptional Activity. *J. Virol.* **2018**, *92*, e00465-18. [CrossRef]
13. James, M.A.; Lee, J.H.; Klingelhutz, A.J. Human papillomavirus type 16 E6 activates NF-kappaB, induces cIAP-2 expression, and protects against apoptosis in a PDZ binding motif-dependent manner. *J. Virol.* **2006**, *80*, 5301–5307. [CrossRef] [PubMed]
14. Güzel, C.; Govorukhina, N.I.; Wisman, G.B.A.; Stingl, C.; Dekker, L.J.; Klip, H.G.; Hollema, H.; Guryev, V.; Horvatovich, P.L.; van der Zee, A.G. Proteomic alterations in early stage cervical cancer. *Oncotarget* **2018**, *9*, 18128. [CrossRef] [PubMed]
15. Pappa, K.I.; Lygirou, V.; Kontostathi, G.; Zoidakis, J.; Makridakis, M.; Vougas, K.; Daskalakis, G.; Polyzos, A.; Anagnou, N.P. Proteomic analysis of normal and cancer cervical cell lines reveals deregulation of cytoskeleton-associated proteins. *Cancer Genomics Proteom.* **2017**, *14*, 253–266.
16. Ding, Y.; Yang, M.; She, S.; Min, H.; Xv, X.; Ran, X.; Wu, Y.; Wang, W.; Wang, L.; Yi, L.; et al. iTRAQ-based quantitative proteomic analysis of cervical cancer. *Int. J. Oncol.* **2015**, *46*, 1748–1758. [CrossRef]
17. Xu, D.; Zhu, X.; Ren, J.; Huang, S.; Xiao, Z.; Jiang, H.; Tan, Y. Quantitative proteomic analysis of cervical cancer based on TMT-labeled quantitative proteomics. *J. Proteom.* **2022**, *252*, 104453. [CrossRef]

18. Garibay-Cerdenares, O.L.; Sánchez-Meza, L.V.; Encarnación-Guevara, S.; Hernández-Ortíz, M.; Martínez-Batallar, G.; Torres-Rojas, F.I.; Mendoza-Catalán, M.Á.; Del Moral-Hernández, O.; Leyva-Vázquez, M.A.; Illades-Aguiar, B. Effect of HPV 16 E6 Oncoprotein Variants on the Alterations of the Proteome of C33A Cells. *Cancer Genomics Proteom.* **2021**, *18*, 273–283. [CrossRef]

19. Merkley, M.A.; Hildebrandt, E.; Podolsky, R.H.; Arnouk, H.; Ferris, D.G.; Dynan, W.S.; Stöppler, H. Large-scale analysis of protein expression changes in human keratinocytes immortalized by human papilloma virus type 16 E6 and E7 oncogenes. *Proteom. Sci.* **2009**, *7*, 29. [CrossRef]

20. Rabilloud, T.; Chevallet, M.; Luche, S.; Lelong, C. Two-dimensional gel electrophoresis in proteomics: Past, present and future. *J. Proteom.* **2010**, *73*, 2064–2077. [CrossRef]

21. Sedman, S.; Barbosa, M.; Vass, W.; Hubbert, N.; Haas, J.; Lowy, D.; Schiller, J. The full-length E6 protein of human papillomavirus type 16 has transforming and trans-activating activities and cooperates with E7 to immortalize keratinocytes in culture. *J. Virol.* **1991**, *65*, 4860–4866. [CrossRef]

22. Barczak, W.; Suchorska, W.; Rubiś, B.; Kulcenty, K. Universal real-time PCR-based assay for lentiviral titration. *Mol. Biotechnol.* **2015**, *57*, 195–200. [CrossRef] [PubMed]

23. Ma, S.; Dai, Y. Principal component analysis based methods in bioinformatics studies. *Brief. Bioinform.* **2011**, *12*, 714–722. [CrossRef] [PubMed]

24. Ritchie, M.E.; Phipson, B.; Wu, D.; Hu, Y.; Law, C.W.; Shi, W.; Smyth, G.K. Limma powers differential expression analyses for RNA-sequencing and microarray studies. *Nucleic Acids Res.* **2015**, *43*, e47. [CrossRef] [PubMed]

25. Benjamini, Y.; Hochberg, Y. Controlling the false discovery rate: A practical and powerful approach to multiple testing. *J. R. Stat. Soc. Ser. B* **1995**, *57*, 289–300. [CrossRef]

26. Szklarczyk, D.; Morris, J.H.; Cook, H.; Kuhn, M.; Wyder, S.; Simonovic, M.; Santos, A.; Doncheva, N.T.; Roth, A.; Bork, P. The STRING database in 2017: Quality-controlled protein–protein association networks, made broadly accessible. *Nucleic Acids Res.* **2017**, *45*, D362–D368. [CrossRef] [PubMed]

27. Engelman, J.A.; Wykoff, C.C.; Yasuhara, S.; Song, K.S.; Okamoto, T.; Lisanti, M.P. Recombinant expression of caveolin-1 in oncogenically transformed cells abrogates anchorage-independent growth. *J. Biol. Chem.* **1997**, *272*, 16374–16381. [CrossRef]

28. Borowicz, S.; van Scoyk, M.; Avasarala, S.; Rathinam, M.K.K.; Tauler, J.; Bikkavilli, R.K.; Winn, R.A. The soft agar colony formation assay. *JoVE* **2014**, *92*, e51998. [CrossRef]

29. Dominguez-Bautista, J.A.; Klinkenberg, M.; Brehm, N.; Subramaniam, M.; Kern, B.; Roeper, J.; Auburger, G.; Jendrach, M. Loss of lysosome-associated membrane protein 3 (LAMP3) enhances cellular vulnerability against proteasomal inhibition. *Eur. J. Cell Biol.* **2015**, *94*, 148–161. [CrossRef]

30. Liu, S.; Yue, J.; Du, W.; Han, J.; Zhang, W. LAMP3 plays an oncogenic role in osteosarcoma cells partially by inhibiting TP53. *Cell. Mol. Biol. Lett.* **2018**, *23*, 33. [CrossRef]

31. Michael, D.; Oren, M. The p53–Mdm2 module and the ubiquitin system. *Semin. Cancer Biol.* **2003**, *13*, 49–58. [CrossRef]

32. Wang, G.; Fersht, A.R. Multisite aggregation of p53 and implications for drug rescue. *Proc. Natl. Acad. Sci. USA* **2017**, *114*, E2634–E2643. [CrossRef] [PubMed]

33. Slebos, R.J.; Jehmlich, N.; Brown, B.; Yin, Z.; Chung, C.H.; Yarbrough, W.G.; Liebler, D.C. Proteomic analysis of oropharyngeal carcinomas reveals novel HPV-associated biological pathways. *Int. J. Cancer* **2013**, *132*, 568–579. [CrossRef] [PubMed]

34. Ndiaye, C.; Mena, M.; Alemany, L.; Arbyn, M.; Castellsagué, X.; Laporte, L.; Bosch, F.X.; de Sanjosé, S.; Trottier, H. HPV DNA, E6/E7 mRNA, and p16INK4a detection in head and neck cancers: A systematic review and meta-analysis. *Lancet Oncol.* **2014**, *15*, 1319–1331. [CrossRef]

35. Moody, C.A.; Laimins, L.A. Human papillomavirus oncoproteins: Pathways to transformation. *Nat. Rev. Cancer* **2010**, *10*, 550–560. [CrossRef] [PubMed]

36. Van Dam, P.A.; van Dam, P.-J.H.; Rolfo, C.; Giallombardo, M.; van Berckelaer, C.; Trinh, X.B.; Altintas, S.; Huizing, M.; Papadimitriou, K.; Tjalma, W.A. In silico pathway analysis in cervical carcinoma reveals potential new targets for treatment. *Oncotarget* **2016**, *7*, 2780. [CrossRef]

37. De Gregorio, V.; Urciuolo, F.; Netti, P.A.; Imparato, G. In Vitro Organotypic Systems to Model Tumor Microenvironment in Human Papillomavirus (HPV)-Related Cancers. *Cancers* **2020**, *12*, 1150. [CrossRef]

38. Bristol, M.L.; Das, D.; Morgan, I.M. Why human papillomaviruses activate the DNA damage response (DDR) and how cellular and viral replication persists in the presence of DDR signaling. *Viruses* **2017**, *9*, 268. [CrossRef]

39. Neves, H.; Kwok, H.F. In sickness and in health: The many roles of the minichromosome maintenance proteins. *Biochim. Biophys. Acta Rev. Cancer* **2017**, *1868*, 295–308. [CrossRef]

40. Giaginis, C.; Vgenopoulou, S.; Vielh, P.; Theocharis, S. MCM proteins as diagnostic and prognostic tumor markers in the clinical setting. *Histol. Histopathol.* **2010**, *25*, 351–370.

41. Das, M.; Prasad, S.B.; Yadav, S.S.; Govardhan, H.; Pandey, L.K.; Singh, S.; Pradhan, S.; Narayan, G. Over expression of minichromosome maintenance genes is clinically correlated to cervical carcinogenesis. *PLoS ONE* **2013**, *8*, e69607. [CrossRef]

42. Li, X.; Tian, R.; Gao, H.; Yan, F.; Ying, L.; Yang, Y.; Yang, P.; Gao, Y.E. Identification of Significant Gene Signatures and Prognostic Biomarkers for Patients With Cervical Cancer by Integrated Bioinformatic Methods. *Technol. Cancer Res. Treat.* **2018**, *17*, 1533033818767455. [CrossRef]

43. Sardo, F.L.; Strano, S.; Blandino, G. YAP and TAZ in Lung Cancer: Oncogenic Role and Clinical Targeting. *Cancers* **2018**, *10*, 137. [CrossRef] [PubMed]

44. Chicas, A.; Wang, X.; Zhang, C.; McCurrach, M.; Zhao, Z.; Mert, O.; Dickins, R.A.; Narita, M.; Zhang, M.; Lowe, S.W. Dissecting the unique role of the retinoblastoma tumor suppressor during cellular senescence. *Cancer Cell* **2010**, *17*, 376–387. [CrossRef] [PubMed]

45. Li, R.; Zhu, J.; Xie, Z.; Liao, G.; Liu, J.; Chen, M.-R.; Hu, S.; Woodard, C.; Lin, J.; Taverna, S.D. Conserved herpesvirus kinases target the DNA damage response pathway and TIP60 histone acetyltransferase to promote virus replication. *Cell Host Microbe* **2011**, *10*, 390–400. [CrossRef]

46. Boichuk, S.; Hu, L.; Hein, J.; Gjoerup, O.V. Multiple DNA damage signaling and repair pathways deregulated by simian virus 40 large T antigen. *J. Virol.* **2010**, *84*, 8007–8020. [CrossRef]

47. Kudoh, A.; Iwahori, S.; Sato, Y.; Nakayama, S.; Isomura, H.; Murata, T.; Tsurumi, T. Homologous recombinational repair factors are recruited and loaded onto the viral DNA genome in Epstein-Barr virus replication compartments. *J. Virol.* **2009**, *83*, 6641–6651. [CrossRef] [PubMed]

48. Zhang, Y.; Fan, S.; Meng, Q.; Ma, Y.; Katiyar, P.; Schlegel, R.; Rosen, E.M. BRCA1 interaction with human papillomavirus oncoproteins. *J. Biol. Chem.* **2005**, *280*, 33165–33177. [CrossRef]

49. Das, D.; Smith, N.; Wang, X.; Morgan, I.M. The deacetylase SIRT1 regulates the replication properties of human papillomavirus 16 E1 and E2. *J. Virol.* **2017**, *10*, e00102-17. [CrossRef]

50. Langsfeld, E.S.; Bodily, J.M.; Laimins, L.A. The deacetylase sirtuin 1 regulates human papillomavirus replication by modulating histone acetylation and recruitment of DNA damage factors NBS1 and Rad51 to viral genomes. *PLoS Pathog.* **2015**, *11*, e1005181. [CrossRef]

51. Hasan, U.A.; Zannetti, C.; Parroche, P.; Goutagny, N.; Malfroy, M.; Roblot, G.; Carreira, C.; Hussain, I.; Müller, M.; Taylor-Papadimitriou, J. The human papillomavirus type 16 E7 oncoprotein induces a transcriptional repressor complex on the Toll-like receptor 9 promoter. *J. Exp. Med.* **2013**, *210*, 1369–1387. [CrossRef]

52. Weichert, W.; Denkert, C.; Noske, A.; Darb-Esfahani, S.; Dietel, M.; Kalloger, S.E.; Huntsman, D.G.; Köbel, M. Expression of class I histone deacetylases indicates poor prognosis in endometrioid subtypes of ovarian and endometrial carcinomas. *Neoplasia* **2008**, *10*, 1021–1027. [CrossRef] [PubMed]

53. Choi, J.H.; Kwon, H.J.; Yoon, B.I.; Kim, J.H.; Han, S.U.; Joo, H.J.; Kim, D.Y. Expression profile of histone deacetylase 1 in gastric cancer tissues. *Jpn. J. Cancer Res.* **2001**, *92*, 1300–1304. [CrossRef] [PubMed]

54. So, D.; Shin, H.-W.; Kim, J.; Lee, M.; Myeong, J.; Chun, Y.-S.; Park, J.-W. Cervical cancer is addicted to SIRT1 disarming the AIM2 antiviral defense. *Oncogene* **2018**, *37*, 5191–5204. [CrossRef] [PubMed]

55. Morgan, I.M.; Das, D.; Bristol, M.; Smith, N.W.; Wang, X.; Pichierri, P. Werner helicase control of human papillomavirus 16 E1–E2 DNA replication is regulated by SIRT1 deacetylation. *mBio* **2019**, *10*, e00263-19.

56. Mine, K.L.; Shulzhenko, N.; Yambartsev, A.; Rochman, M.; Sanson, G.F.; Lando, M.; Varma, S.; Skinner, J.; Volfovsky, N.; Deng, T. Gene network reconstruction reveals cell cycle and antiviral genes as major drivers of cervical cancer. *Nat. Commun.* **2013**, *4*, 1806. [CrossRef] [PubMed]

57. Kanao, H.; Enomoto, T.; Kimura, T.; Fujita, M.; Nakashima, R.; Ueda, Y.; Ueno, Y.; Miyatake, T.; Yoshizaki, T.; Buzard, G.S.; et al. Overexpression of LAMP3/TSC403/DC-LAMP promotes metastasis in uterine cervical cancer. *Cancer Res.* **2005**, *65*, 8640–8645. [CrossRef]

58. Liao, X.; Chen, Y.; Liu, D.; Li, F.; Li, X.; Jia, W. High expression of LAMP3 is a novel biomarker of poor prognosis in patients with esophageal squamous cell carcinoma. *Int. J. Mol. Sci.* **2015**, *16*, 17655–17667. [CrossRef]

59. Wang, D.; Cao, X.; Zhang, Y.; Liu, Y.; Yao, C.; Ge, W.; Xu, Y. LAMP3 expression correlated with poor clinical outcome in human ovarian cancer. *Tumor Biol.* **2017**, *39*, 1010428317695014. [CrossRef]

60. Liao, X.; Song, L.; Zhang, L.; Wang, H.; Tong, Q.; Xu, J.; Yang, G.; Yang, S.; Zheng, H. LAMP3 regulates hepatic lipid metabolism through activating PI3K/Akt pathway. *Mol. Cell. Endocrinol.* **2018**, *470*, 160–167. [CrossRef]

61. Bego, M.G.; Mercier, J.; Cohen, É.A. Virus-activated interferon regulatory factor 7 upregulates expression of the interferon-regulated BST2 gene independently of interferon signaling. *J. Virol.* **2012**, *86*, 3513–3527. [CrossRef]

62. Cao, W.; Bover, L.; Cho, M.; Wen, X.; Hanabuchi, S.; Bao, M.; Rosen, D.B.; Wang, Y.-H.; Shaw, J.L.; Du, Q. Regulation of TLR7/9 responses in plasmacytoid dendritic cells by BST2 and ILT7 receptor interaction. *J. Exp. Med.* **2009**, *206*, 1603–1614. [CrossRef]

63. Cai, D.; Cao, J.; Li, Z.; Zheng, X.; Yao, Y.; Li, W.; Yuan, Z. Up-regulation of bone marrow stromal protein 2 (BST2) in breast cancer with bone metastasis. *BMC Cancer* **2009**, *9*, 102. [CrossRef] [PubMed]

64. Fang, K.H.; Kao, H.K.; Chi, L.M.; Liang, Y.; Liu, S.C.; Hseuh, C.; Liao, C.T.; Yen, T.C.; Yu, J.S.; Chang, K.P. Overexpression of BST2 is associated with nodal metastasis and poorer prognosis in oral cavity cancer. *Laryngoscope* **2014**, *124*, E354–E360. [CrossRef] [PubMed]

65. Yokoyama, T.; Enomoto, T.; Serada, S.; Morimoto, A.; Matsuzaki, S.; Ueda, Y.; Yoshino, K.; Fujita, M.; Kyo, S.; Iwahori, K. Plasma membrane proteomics identifies bone marrow stromal antigen 2 as a potential therapeutic target in endometrial cancer. *Int. J. Cancer* **2013**, *132*, 472–484. [CrossRef] [PubMed]

66. Wong, Y.; Cheung, T.; Lo, K.; Yim, S.; Siu, N.; Chan, S.; Ho, T.; Wong, K.; Yu, M.; Wang, V. Identification of molecular markers and signaling pathway in endometrial cancer in Hong Kong Chinese women by genome-wide gene expression profiling. *Oncogene* **2007**, *26*, 1971. [CrossRef] [PubMed]

67.　Mukai, S.; Oue, N.; Oshima, T.; Mukai, R.; Tatsumoto, Y.; Sakamoto, N.; Sentani, K.; Tanabe, K.; Egi, H.; Hinoi, T. Overexpression of transmembrane protein BST2 is associated with poor survival of patients with esophageal, gastric, or colorectal cancer. *Ann. Surg. Oncol.* **2017**, *24*, 594–602. [CrossRef]

68.　Ahn, W.S.; Bae, S.M.; Lee, J.M.; Namkoong, S.E.; Han, S.J.; Cho, Y.L.; Nam, G.H.; Seo, J.S.; Kim, C.K.; Kim, Y.W. Searching for pathogenic gene functions to cervical cancer. *Gynecol. Oncol.* **2004**, *93*, 41–48. [CrossRef]

69.　Sayeed, A.; Luciani-Torres, G.; Meng, Z.; Bennington, J.L.; Moore, D.H.; Dairkee, S.H. Aberrant regulation of the BST2 (Tetherin) promoter enhances cell proliferation and apoptosis evasion in high grade breast cancer cells. *PLoS ONE* **2013**, *8*, e67191. [CrossRef]

70.　Mahauad-Fernandez, W.D.; Okeoma, C.M. Cysteine-linked dimerization of BST-2 confers anoikis resistance to breast cancer cells by negating proapoptotic activities to promote tumor cell survival and growth. *Cell Death Dis.* **2017**, *8*, e2687. [CrossRef]

71.　Ronco, L.V.; Karpova, A.Y.; Vidal, M.; Howley, P.M. Human papillomavirus 16 E6 oncoprotein binds to interferon regulatory factor-3 and inhibits its transcriptional activity. *Genes Dev.* **1998**, *12*, 2061–2072. [CrossRef]

72.　Karim, R.; Tummers, B.; Meyers, C.; Biryukov, J.L.; Alam, S.; Backendorf, C.; Jha, V.; Offringa, R.; van Ommen, G.J.; Melief, C.J.; et al. Human papillomavirus (HPV) upregulates the cellular deubiquitinase UCHL1 to suppress the keratinocyte's innate immune response. *PLoS Pathog.* **2013**, *9*, e1003384. [CrossRef] [PubMed]

73.　Rayet, B.; Gelinas, C. Aberrant rel/nfkb genes and activity in human cancer. *Oncogene* **1999**, *18*, 6938. [CrossRef]

74.　Moon, H.S.; Park, H.M.; Chung, H.W. The midkine mRNA expression in invasive cervical cancer. *Korean J. Gynecol. Oncol. Colposc.* **2000**, *11*, 123–130. [CrossRef]

75.　O'Brien, T.; Cranston, D.; Fuggle, S.; Bicknell, R.; Harris, A.L. The angiogenic factor midkine is expressed in bladder cancer, and overexpression correlates with a poor outcome in patients with invasive cancers. *Cancer Res.* **1996**, *56*, 2515–2518. [PubMed]

76.　Shimada, H.; Nabeya, Y.; Okazumi, S.-I.; Matsubara, H.; Kadomatsu, K.; Muramatsu, T.; Ikematsu, S.; Sakuma, S.; Ochiai, T. Increased serum midkine concentration as a possible tumor marker in patients with superficial esophageal cancer. *Oncol. Rep.* **2003**, *10*, 411–414. [CrossRef] [PubMed]

77.　Zhao, Z.-Q.; Yang, S.; Lu, H.-S. Expression of midkine and vascular endothelial growth factor in gastric cancer and the association of high levels with poor prognosis and survival. *Mol. Med. Rep.* **2012**, *5*, 415–419. [PubMed]

78.　Owada, K.; Sanjo, N.; Kobayashi, T.; Mizusawa, H.; Muramatsu, H.; Muramatsu, T.; Michikawa, M. Midkine inhibits caspase-dependent apoptosis via the activation of mitogen-activated protein kinase and phosphatidylinositol 3-kinase in cultured neurons. *J. Neurochem.* **1999**, *73*, 2084–2092.

79.　Stoica, G.E.; Kuo, A.; Powers, C.; Bowden, E.T.; Sale, E.B.; Riegel, A.T.; Wellstein, A. Midkine binds to anaplastic lymphoma kinase (ALK) and acts as a growth factor for different cell types. *J. Biol. Chem.* **2002**, *277*, 35990–35998. [CrossRef]

80.　Fukazawa, T.; Maeda, Y.; Yamatsuji, T.; Takaoka, M.; Yoshida, M.; Ishida, N.; Iwai, M.; Yokota, E.; Yukawa, T.; Haisa, M. Development of a novel targeted therapy for malignant mesothelioma carcinoma by a midkine inhibitor. *Cancer Res.* **2017**, *77* (Suppl. 13), 2085. [CrossRef]

81.　Duffy, C.L.; Phillips, S.L.; Klingelhutz, A.J. Microarray analysis identifies differentiation-associated genes regulated by human papillomavirus type 16 E6. *Virology* **2003**, *314*, 196–205. [CrossRef]

82.　Rheinwald, J.G.; Beckett, M.A. Defective terminal differentiation in culture as a consistent and selectable character of malignant human keratinocytes. *Cell* **1980**, *22*, 629–632. [CrossRef]